NanoImpact 42 (2026) 100631

Contents lists available at ScienceDirect

NanoImpact

journal homepage: www.elsevier.com/locate/nanoimpact

Research Paper

Using simple to more robust *in vitro* methods based on human pulmonary models to evaluate the acute and subacute toxicity of micro- and nanoplastics derived from 3D printing materials☆

Itziar Polanco-Garriz [a], Juliana Carrillo-Romero [a], Mari Venäläinen [b], Jussi Lyyränen [b], Hanna Pulli [b], Satu Suhonen [b], Jolanda Vermeulen [c], Nienke Ruijter [c], Ana Candalija Iserte [d], Apostolos Salmatonidis [d], Marie Carriere [e], Morgan Lofty [f], Matthew Boyles [f,g], Davide Lotti [h], Jesús C. Guzmán-Mínguez [i,j], José F. Fernández [i], Flemming Cassee [c,k], Julia Catalán [b,l], Isabel Rodríguez-Llopis [a], Socorro Vázquez-Campos [d], Felipe Goñi de Cerio [a], Alberto Katsumiti [a,*]

[a] *GAIKER Technology Centre, Basque Research and Technology Alliance (BRTA), Zamudio, Spain*
[b] *Finnish Institute of Occupational Health (FIOH), Helsinki, Finland*
[c] *National Institute for Public Health and the Environment (RIVM), Bilthoven, the Netherlands*
[d] *Leitat Technological Center, Barcelona, Spain*
[e] *Univ. Grenoble Alpes, CEA, CNRS, Grenoble-INP, IRIG, SyMMES-CIBEST, F-38000 Grenoble, France*
[f] *Institute of Occupational Medicine (IOM), Edinburgh, United Kingdom*
[g] *Centre for Biomedicine and Global Health, School of Applied Sciences, Edinburgh Napier University, Edinburgh, United Kingdom*
[h] *LATI Thermoplastic Industry S.p.A., Vedano Olona, Italy*
[i] *Instituto de Ceramica y Vidrio, ICV-CSIC, Madrid, Spain*
[j] *Universidad Antonio Nebrija, C/ Santa Cruz de Marcenado (Campus Madrid-Princesa), 28015 Madrid, Spain*
[k] *Institute for Risk Assessment Sciences (IRAS), Utrecht, the Netherlands*
[l] *Department of Anatomy, Embryology and Genetics, University of Zaragoza, Zaragoza, Spain*

ARTICLE INFO

Editor: Phil Demokritou

Keywords:
Toxicity
In vitro
Robust model
Simple model
Subacute
Pulmonary
3D printing

ABSTRACT

Mechanical recycling and other processes involved in the end-of-life treatment of 3D-printed plastic polymers can lead to the generation of micro- and nanoplastics (MNPs). As the use of these materials continues to grow, the mechanical degradation of plastics from 3D printing may increase human exposure to MNPs, raising concerns about potential health risks for users and environmental impacts. One of the main routes of exposure to MNPs is *via* inhalation. For regulatory purposes, most of inhalation studies have been performed using rodents and following the OECD TG 412, however, these models do not accurately mimic the physiology of the human pulmonary system. As alternative, New Approach Methodologies (NAMs) based on human *in vitro* models have been used lately, providing simple and valuable, and physiologically relevant tools for research. In this work, simple *in vitro* models using Calu-3 and TK6 cells were exposed for 24 h (acute) and the advanced primary human epithelial MucilAir™ model was exposed for 24 h (acute) and 28 days (sub-acute, adapting the OECD TG 412) to MNPs made of polypropylene (PP), polycarbonate (PC), PP + silver nanoparticles (PP + Ag) and PC + single wall carbon nanotubes (PC + SWCNT). The results showed no significant toxicity of MNPs in acute exposures using the Calu-3 and TK6 models. In contrast, significant effects were observed along time after acute and subacute exposure of MucilAir™ to the different MNPs. These results indicate that robust *in vitro* models such as MucilAir™ may represent a valuable NAM for acute and sub-acute inhalation toxicity studies.

☆ This article is part of a Special issue entitled: 'MNPs: Fate and hazards in Human' published in NanoImpact.

* Corresponding author.
E-mail address: katsumiti@gaiker.es (A. Katsumiti).

https://doi.org/10.1016/j.impact.2026.100631
Received 28 November 2025; Received in revised form 17 March 2026; Accepted 11 May 2026
Available online 14 May 2026

1. Introduction

In the last years, 3D printing has emerged as a useful technology to produce complex 3D structures with a wide range of industrial and consumer applications. Among industrial applications, 3D printing is highly useful to produce medical devices like dental or orthopedic implants or microfluidic chips, as well as to customize those pieces according to the patient. It can also be employed for tissue engineering to create tissues and organs improving transplant success rates, as well as in other biomedical areas like biosensing, immunotherapy or drug delivery (Shiva et al., 2023). Furthermore, 3D printing can also be used in food industry or to produce consumer products such as replacement parts, household items or toys (Kwon et al., 2017; Sigloch et al., 2020; Vallabani et al., 2022; Velásquez-García and Kornbluth, 2025). Thermoplastics like acrylonitrile butadiene styrene (ABS), polylactic acid (PLA), Nylon, polypropylene (PP) and polycarbonate (PC) are commonly used in 3D printing.

PP is one of the most significant plastic materials for 3D printing due to its compatibility with the printing process, and it is becoming a sustainable alternative to other conventional plastic materials due to low waste rates (Kristiawan et al., 2021; Shiva et al., 2023). PP shows interesting characteristics such as chemical resistance and low density (Kristiawan et al., 2021; Ludwicka et al., 2018; Shiva et al., 2023; Sigloch et al., 2020), useful for 3D printing, as well as in the biomedical fields as it can be sterilized (Shiva et al., 2023). However, this material is not biodegradable, implying that it can persist in the body and in the environment for a long time, which could become a risk for human and environmental health (Shiva et al., 2023).

PC is also frequently used in 3D printing since it presents excellent thermal, mechanical and optical properties (Makki et al., 2024). It shows high compatibility with other polymers and additives. It can be used in electronics, building or automotive sector, and in biomedical fields due to having good biocompatibility with *in vitro* and *in vivo* systems, to generate scaffolds for tissue engineering and drug delivery systems. However, PC is also non-biodegradable, which implies that it may be accumulated in the environment and human body, leading to adverse health effects (Shiva et al., 2023).

Nanomaterials are increasingly used in 3D printing to enhance material properties and enable new applications. By incorporating nanomaterials, researchers are developing printed components, also called nano-enabled products (NEPs), with enhanced electrical conductivity, mechanical strength, and biocompatibility. Single wall carbon nanotubes (SWCNT) or silver nanoparticles (Ag NPs) can be used in combination with PC and PP matrices, respectively, to enhance the material properties of PC and PP (Kristiawan et al., 2021; Shiva et al., 2023). SWCNTs can be added to polymeric filaments to increase antistatic properties of the final product. Ag NPs have recently attracted interests due to their antibacterial properties. However, these additive materials present significant human and environmental risks related to some of their properties (Jiang et al., 2020; Wāng et al., 2024).

Recycling of 3D printed waste is also considered as a source of plastic exposure. The most widespread technology for large-scale recycling of plastic waste is currently mechanical abrasion (Schwarz et al., 2021; Suzuki et al., 2022), which implies several stages: first, the waste is sorted by type (*e.g.*, PLA, ABS) and colour, with contaminants like glue or metal removed manually. The large parts are then shredded into smaller secondary particles (including MNPs). These particles are washed to remove impurities and dried to prevent issues during extrusion. Finally, the cleaned particles are melted and extruded into filament, which is spooled onto a roll, with systems in place to ensure consistent diameter throughout the process. Therefore, during the lifecycle of the waste plastic materials produced by 3D printing secondary particles are released into the air, leading to potential human exposure (Wade et al., 2023; Zhang and Black, 2023; Zhou et al., 2023). Therefore, mechanical recycling of 3D-printed pieces has become a worldwide health concern related to the potential hazard of these particles and VOCs to human health, specially to users (Arrizubieta et al., 2020; Schwarz et al., 2021; Suzuki et al., 2022; Vallabani et al., 2022).

Various studies have reported that workers regularly exposed to MNPs released during mechanical recycling of 3D printing waste show respiratory symptoms, *i.e.*, shortness of breath, coughing, chest tightness, as well as other symptoms like eye and nose irritation due to the inhalation of these particles, which could indicate damage to the lung tissue (Karlsson et al., 2008; Lisiecki et al., 2024; Zhou et al., 2023). In fact, added NPs such as metal NPs or carbon nanotubes (CNTs) showed cytotoxic effects and caused DNA damage on *in vitro* pulmonary models (Karlsson et al., 2008; Sigloch et al., 2020).

For inhalation studies, standard guidelines such as the OECD TG 412 have been widely used for subacute (28 days) inhalation toxicity assessment (Casati, 2018; Mercier et al., 2019; Miller and Spence, 2017; Pauluhn and Mohr, 2000). Despite the great applicability of this *in vivo*-based guideline, animal testing does not always provide relevant information for human health assessment. Although *in vivo* models might be necessary in some cases to support *in vitro* toxicity assessment, it is known that animal and human lung physiology show large differences, which complicates inferring how animal studies could be applied to human health (Casati, 2018; Mercier et al., 2019; Miller and Spence, 2017). For instance, lungs in rodents develop quickly, starting at embryonic day 9, but form alveoli structures after birth; whereas in the human body this development occurs in additional phases from week 3 up to 3 years after birth, including the formation of branching before the alveolarization (Miller and Spence, 2017; Rackley and Stripp, 2012). In addition, stem cell and progenitor cell populations are widely different between rodent and human lungs and the localization of the different cell populations in the respiratory system varies (Miller and Spence, 2017). Additionally, the respiratory system is defined by genetic variability, and, during the human adult phase, it is exposed to external factors such as environmental pollution or individual lifestyle, which cannot be considered when using a rodent model. Regarding the study of the respiratory system, it has been shown that rodents may show higher sensitivity to certain chemicals than humans (Doke and Dhawale, 2015; García-Salvador et al., 2021; Ito et al., 2020; Miller and Spence, 2017; van der Zalm et al., 2022).

To overcome these issues, various New Approach Methodologies (NAMs) based on *in silico* and/or human-based *in vitro* methods have been used lately (Doke and Dhawale, 2015; García-Salvador et al., 2021; Ito et al., 2020; Miller and Spence, 2017; Petersen et al., 2023; van der Zalm et al., 2022; Yang et al., 2023b). Human cell lines such as Calu-3 and TK6 offer an attractive alternative to animal experimentation, providing a simple and valuable tool for research. These models allow for a controlled cellular environment that can be monitored in real time. Additionally, pulmonary cell lines can be cultured at the air-liquid interface (ALI) to promote the differentiation of cells with mucociliary functions, enabling the study of the epithelial pulmonary barrier (Miller and Spence, 2017). This technique leads to the polarization of human ciliated and mucus-producing cells, giving them apical-basal morphology, functional apical cilia and mucus secretion from goblet cells. However, these simplified models only offer a partial representation of the human pulmonary system. Additionally, whether cells are immortalized or transformed, it remains unclear how well they maintain the physiological characteristics of normal airway cells. This limitation constitutes a significant challenge in developing more complex and accurate *in vitro* human models based on human cell lines (Becker and Sadayappan, 2020; Miller and Spence, 2017).

Advanced *in vitro* models based on complex three-dimensional systems are being developed to mimic the *in vivo* microenvironment more realistically. Lung tissues based on human primary bronchial epithelial cells (PBEC) such as the bronchial model MucilAir™ (Epithelix) represent an alternative to animal models as they consist of primary cells, and can be used in acute and subacute studies, remaining for up to 6 months in culture conditions without losing biological response and physiological features (Cervena et al., 2019; Ito et al., 2020; Rossner et al., 2019).

MucilAir™ model is mainly composed of bronchial cells – basal, goblet and ciliated cells - maintaining some key tissue features such as the cell-to-cell interactions of the bronchial epithelium, production of mucous and ciliary movement (Cervena et al., 2019; Tratnjek et al., 2021). Therefore, it represents a fully differentiated and functional respiratory epithelium that may accurately reproduce the biophysiology of human airway epithelium (Cervena et al., 2019; Mercier et al., 2019).

In this study, particular attention was given to MNPs generated through mechanical recycling of 3D printed materials made of PC and PP, with or without the addition of SWCNTs and Ag NPs, respectively. To investigate their potential adverse pulmonary effects, simple *in vitro* models using Calu-3 and TK6 cells were employed to assess acute (24-h) responses. In parallel, a more advanced system was used to examine both acute (24 h) and sub-acute (up to 28 days) effects, following an adapted OECD TG 412 framework in which the traditional *in vivo* rodent model is replaced by the *in vitro* primary human bronchial epithelial model (MucilAir™).

2. Materials and methods

2.1. Acquisition, characterization and reactivity of the MNPs

To simulate mechanical recycling of the 3D printed materials, four 3D objects made of PC, PC + SWCNT, PP and PP + Ag printed using FDM of thermoplastic filaments manufactured by the LATI3DLab division of LATI Industria Termoplastici S.p.A. (LATI3DLab). Acquisition and characterization of MNPs are fully described in Rodríguez-Garraus et al. (2025). Briefly, the MNPs were obtained through a three-stage top-down process. First, the 3D-printed objects were subjected to micro-scale cryogenic grinding using a PULVERISETTE 11 laboratory blade mill (FRITSCH GmbH, Idar-Oberstein, Germany), operated for 2 min at 3600 rpm. Subsequently, the resulting micrometric particles were processed by high-energy mechanical grinding in an aqueous medium for a total of 45 min, distributed over three 15-min cycles, at a rotation speed of 420 rpm, in order to obtain particles smaller than 50 μm. Finally, the particles obtained were sieved through a 5 μm mesh to isolate the fraction with a size <5 μm, considered relevant from a toxicological point of view as it corresponds to the size threshold associated with cellular absorption (Champion et al., 2008; Yang et al., 2023a). This method is suitable for the generation of MNPs based on PP and PC materials, which constitute secondary particles potentially generated during recycling of 3D printing waste.

MNPs were characterized using a Jeol JEM-1400 Flash transmission electron microscope (TEM) with a Jeol Dry SD30GV energy dispersive X-ray (EDX) detector using 80 kV accelerating voltage to analyse morphology, size and chemical composition. In addition, PC and PC + SWCNT samples were analysed using the Thermo Scientific DXR3 Raman microscope to verify the presence of SWCNT particles (Rodríguez-Garraus et al., 2025). To determine the average particle size and polydispersity index (PDI) dynamic light scattering (DLS) was used (Rodríguez-Garraus et al., 2025). MNPs were suspended in 0.05% BSA-water (BSA, Sigma A2934) and in culture medium (DMEM/F12) as dispersants. In addition, to determine the surface charge of the particles, *Z*-potential was measured.

To further assess the oxidative potential of the materials in an acellular system, reactivity of MNPs was analysed using the ferric reducing ability of serum (FRAS) assay (Ruijter et al., 2024). This assay indirectly measures potential reactive oxygen species (ROS) generation in human blood serum (HBS), by calculating the total antioxidant depletion in HBS after exposure to the MNPs. As stated in Ruijter et al. (2024), MNP materials were weighted in glass vials where 1.5 mL of HBS was added before dispersion in a ultrasonicator bath. CuO nanoparticles (34.5 g/L, 50 nm, Sigma Aldrich 544,868) were used as positive control due to their high oxidative potential. $BaSO_4$ (30.3 g/L, 31.5 nm, JRC Nanomaterials Repository, NM220-JRCNM50001) were used as negative control. Samples were then incubated for 3 h in the dark at 37 °C with agitation 300 rpm. Afterwards, samples were centrifugated for 2.5 h at 14000 x g at 4 °C to recover the supernatants. Supernatants were transferred to a 96-well plate in triplicate and mixed with FRAS reagent containing ferric ions (Fe^{3+}) and 4,6-tripyridyl-*s*-triazine (TPTZ). The remaining antioxidants in the HBS reduced Fe^{3+} to Fe^{2+} forming a Fe^{2+}–TPTZ complex with a bright blue colour. FRAS reagents and the Trolox standard curve were prepared following the original protocol described in Gandon et al. (2017). Samples were incubated for 1 h in the dark with agitation at room temperature before measuring absorbance at 593 nm. The reactivity potential of the materials was calculated as the biological oxidative damage (BOD) and expressed in Trolox equivalent units (TEU) using a standard curve with increasing concentrations of Trolox (water soluble vitamin E analogue) as a calibrator.

2.2. MNP exposures

For the exposure of Calu-3 and acute *in vitro* exposure, the obtained MNPs were weighted and serially diluted in serum-free culture medium. For the exposure of TK6 acute and MucilAir acute and sub-acute *in vitro* exposures, the obtained MNPs were weighted and serially diluted in complete culture medium. Before exposing the cells, the suspensions were vortexed thoroughly between dilutions steps and before exposures. Cells were then exposed at quasi-ALI conditions. Details are provided below.

2.3. Cell models

The epithelial lung adenocarcinoma Calu-3 cell line was chosen as a Tier 2 (simple, cost-effective and easy-to-use) *in vitro* human bronchial model. This cell line has been reported as suitable to retain its monolayer structure and develop strong tight junctions under long-term ALI conditions, key for a biological barrier model (He et al., 2021). This cell line was purchased from ATCC and cultured in MEM-Glutamax (Gibco, 42360–081) with 10% Fetal Bovine Serum (FBS, Gibco, 1050064), 1% non-essential aminoacids (NEAA, Gibco, 11140–035) and 1% penicillin/streptomycin (Gibco, 15140122) and maintained at 37 °C and 5% CO_2 atmosphere, according to the manufacturer.

The human non-cancerous lymphoblastoid-B TK6 cell line was chosen to perform micronucleus assay. This cell line is derived from a 5-year-old male with hereditary spherocytosis, a non-cancerous blood disorder, with high interest in research due to the genetic properties of these cells. Among these properties, wild-type p53 and heterozygosity at the thymidine kinase (TK) locus may be highlighted, making them excellent models for studying mutations and genotoxicity. In addition, TK6 cell line is recommended to perform the micronucleus assay according to the adapted OECD TG 487 for testing nanomaterials (OECD, 2023). TK6 cell line was purchased European Collection of Authenticated Cell Cultures (ECACC) and cultured in Roswell Park Memorial Institute (RPMI-1640) medium (ThermoFisher) supplemented with 1% L-glutamine (2 mM; HyClone products), 1% sodium pyruvate (1 mM; HyClone products) and 10% horse serum (HyClone products) and incubated at 37 °C in a humidified atmosphere with 5% CO_2, in an upright position, on a shaker plate (60 rpm).

The MucilAir™ model was chosen as a Tier 3 (complex, robust, realistic) *in vitro* human bronchial model. MucilAir™ inserts, ready-to-use culture media (MucilAir™ Culture Media, Epithelix) and supplements were purchased from Epithelix (Geneva, Switzerland). Inserts, coming from 3 healthy donors (2 females and 1 male, ages 42 to 64), were treated separately as 3 biological replicates. Upon receiving inserts and following provider's instructions, tissues were washed once with 200 μL of cell culture medium and maintained at 37 °C and 5% CO_2 in culture medium (basolateral only) for 7 days with basolateral medium renewal every 2–3 days. The apical part of the inserts was kept at air-liquid interface (ALI) and washed once with 200 μL of PBS every 2–3 days to remove the excess of mucous.

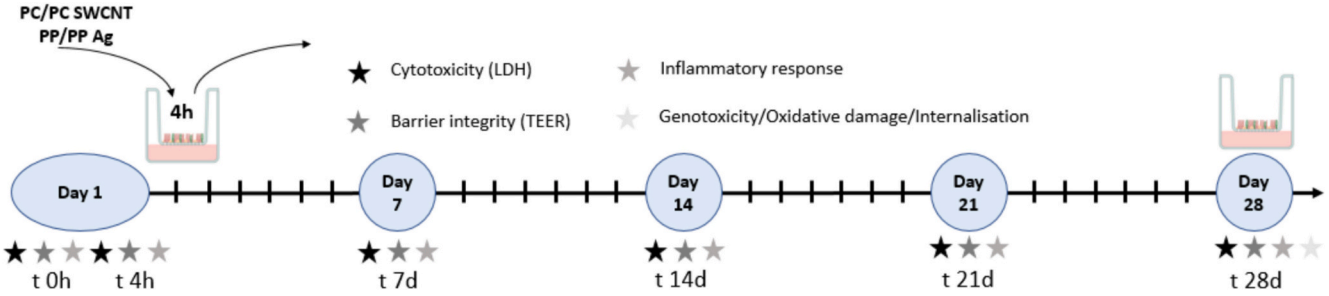

Fig. 1. Exposure of MucilAir model to PC, PC + SWCNT, PP and PP + Ag MNPs and collection of samples at time 0 and 4 h, and at days 7, 14, 21 and 28. Inserts were exposed to 20 µL of the MNPs for 4 h/day, 5 days a week (Monday to Friday), with an apical wash after the exposure time. Basolateral medium was renewed every 2 days.

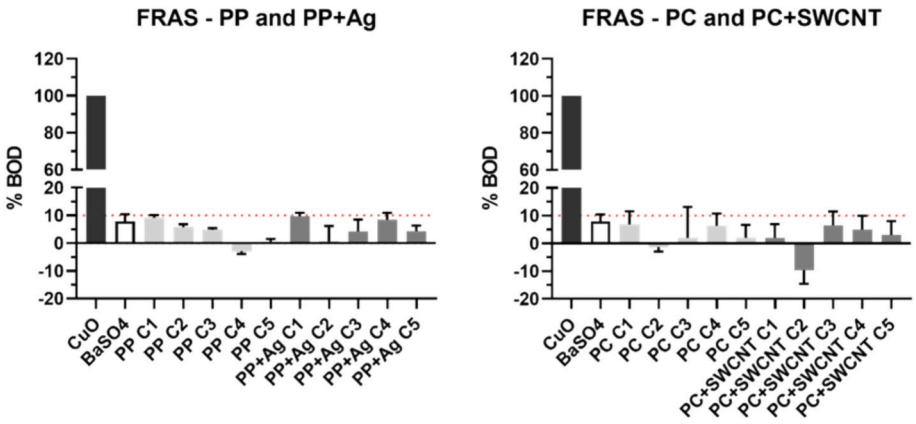

Fig. 2. Oxidative potential (FRAS assay) of PC, PC + SWCNT, PP and PP + Ag MNPs. The MNP materials were tested in a range of increasing concentrations (0.75, 2, 5.5, 15 and 40 g/L from C1 to C5). CuO and $BaSO_4$ nanoparticles were used as positive and negative controls, both tested at dose 1 m^2/mL corresponding to 34.5 and 30.3 g/L, respectively. Results are expressed as mean value ± SE of 2 replicates per tested condition.

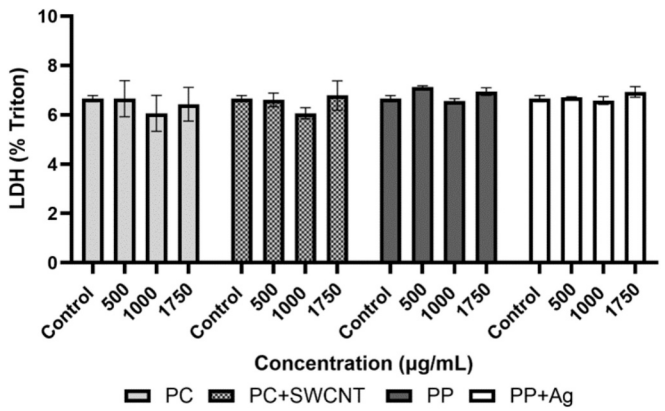

Fig. 3. Cytotoxicity (LDH assay) of Calu-3 model exposed to 500, 1000 and 1750 µg/mL of PC, PC + SWCNT, PP and PP + Ag MNPs for 24 h. Results are expressed as mean value ± SE of 3 replicates per tested condition in respect to positive control (Triton X-100). $N = 3$. Symbols indicate significant differences with respect to the untreated control cells ($p < 0.05$).

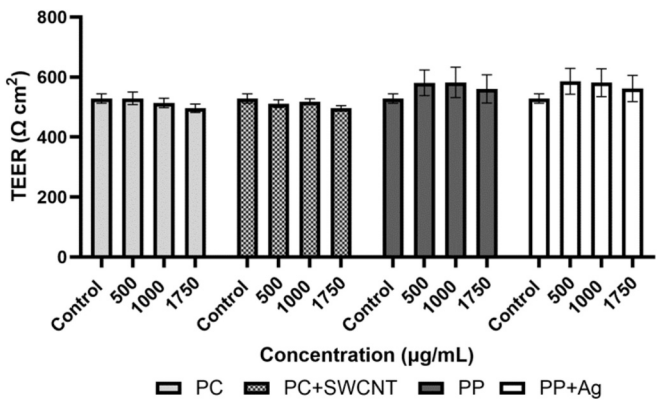

Fig. 4. Cell barrier integrity through transepithelial electric resistance (TEER) of Calu-3 model exposed to 500, 1000 and 1750 µg/mL of PC, PC + SWCNT, PP and PP + Ag MNPs for 24 h. Results are expressed as TEER values ± SE of 3 replicates per tested condition. N = 3. Symbols indicate significant differences with respect to the untreated control cells (p < 0.05).

2.4. Acute and subacute exposures

2.4.1. TK6 model

Following the methodology from Burgum et al. (2024), TK6 cells were seeded at 5×10^4 cells/mL in 14 mL cell culture tubes and maintained in continuous rotation. After 1.5-cell cycle (21*h*), cells were exposed for another 1.5-cell cycle to 3.125, 6.25, 12.5, 25 and 50 µg/mL of PC, PC + SWCNT, PP and PP + Ag MNPs (sublethal concentrations selected based on cell viability assay). These concentrations were chosen based on the methodology followed (Burgum et al., 2024), not exceeding 100 µg/mL to avoid agglomeration and minimize the use of non-physiologically relevant doses. Cells were also treated with 0.025 µg/mL of mitomycin C (MMC; Sigma Aldrich) as positive control, and the corresponding interference controls (as recommended by Franz et al., 2020). Untreated cells served as negative control cultures. Each treatment was carried out in triplicate, each of which was measured twice. After exposure, TK6 cells were centrifuged, washed twice with

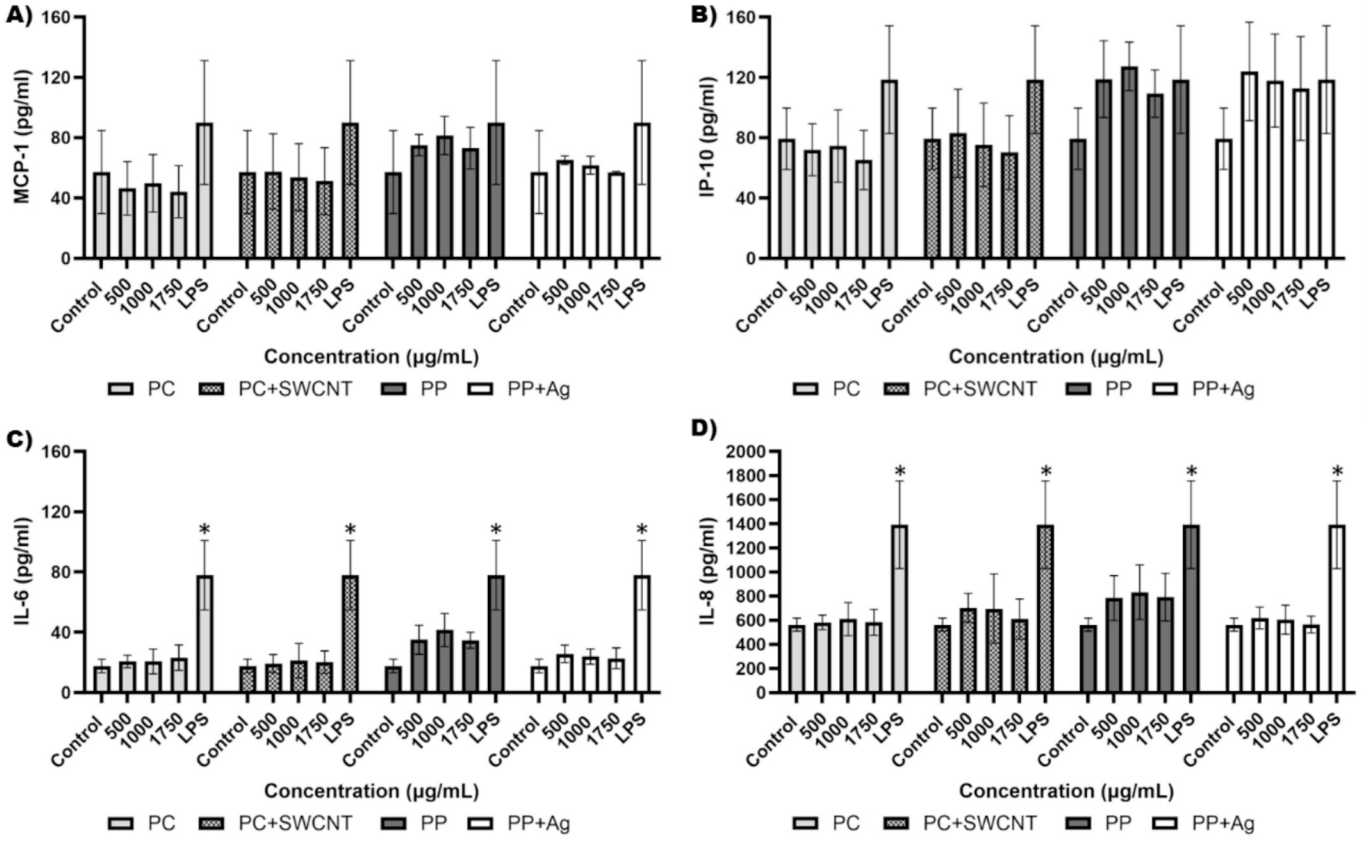

Fig. 5. Inflammatory response (A) MCP-1, B) IP-10, C) IL-6 and D) IL-8) in Calu-3 cells exposed to 500, 1000 and 1750 µg/mL of PC, PC + SWCNT, PP and PP + Ag MNPs for 24 h. Results are expressed as mean value ± SE of 3 replicates per tested condition. $N = 3$. Symbols indicate significant differences with respect to the untreated control cells at the same timepoints ($p < 0.05$).

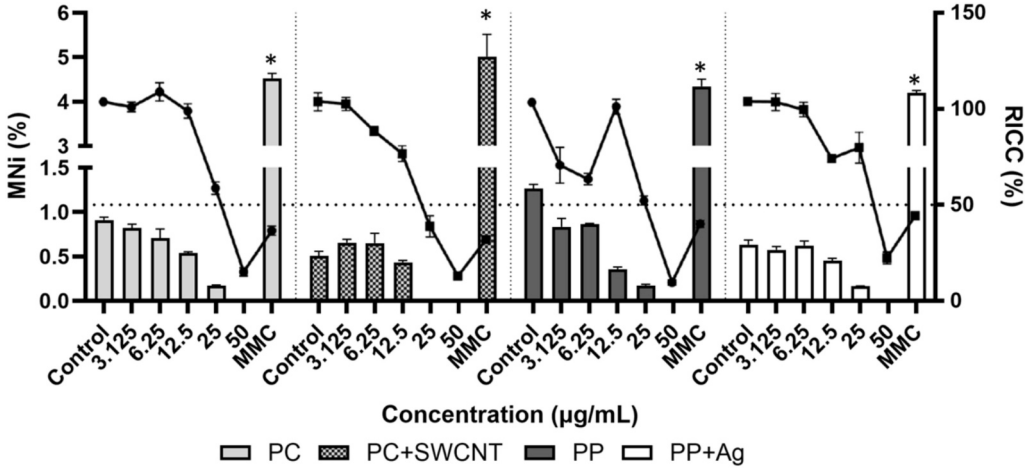

Fig. 6. Micronucleus analysis on TK6 cells exposed to 3.125, 6.25, 12.5, 25 and 50 µg/mL of PC, PC + SWCNT, PP and PP + Ag MNPs for 21 h (1.5-cell cycle). Relative Increase of Cell Count (RICC %), represented in scatter plot (Right Y axis) with 45 ± 5% RICC showed as dotted line. Percentage of micronuclei (MNi %) represented in bars (Left Y axis). Results are expressed as mean value ± SE of 3 replicates per tested condition. N = 3. Symbols indicate significant differences with respect to the untreated control cells at the same timepoints ($p < 0.05$). Positive control Mitomycin C (MMC) was used at 0.025 µg/mL.

phosphate buffered saline (PBS; ThermoFisher) and allowed to recover in complete culture medium for 1.5-cell cycle (21 h).

2.4.2. Calu-3 model

Calu-3 cells were seeded at 2.24×10^5 cells/mL on 0.4 µm pore sized transparent inserts (12 mm diameter, Corning 3460), adding 500 µL of cell suspension in the apical compartment of the inserts and 1.5 mL of complete culture medium in the basolateral compartment. Cells were incubated at 37 °C, 5% CO_2 atmosphere and both apical and basolateral culture media were changed every 2–3 days. At day 8, confluency of the cells was checked, and apical medium was removed, leaving the cell culture in ALI conditions. At day 13 cells were washed with a saline solution (HBSS, H4891 Sigma-Aldrich) in the apical compartment. Finally, at day 15, the pulmonary model was exposed to 500, 1000 and

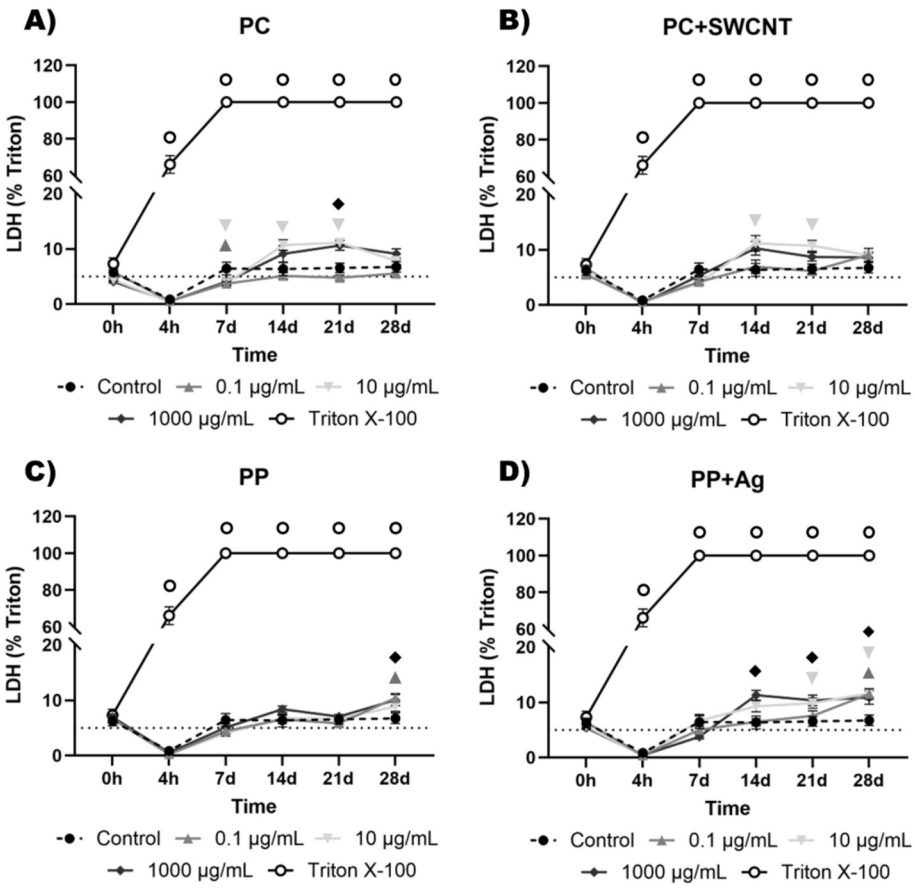

Fig. 7. Cytotoxicity (LDH assay) of MucilAir™ exposed to 0.1, 10 and 1000 µg/mL of A) PC, B) PC + SWCNT, C) PP and D) PP + Ag MNPs for 4 h a day, 28 days. Results are expressed as mean value ± SE of 5 replicates per tested condition in respect to positive control (Triton X-100). $N = 3$. 5% threshold of LDH release is established to determine the health of the MucilAir™ tissue. Symbols indicate significant differences with respect to the untreated control cells at the same timepoint ($p < 0.05$).

1750 µg/mL (corresponding to 8.93, 17.86 and 31.25 µg/cm^2) of PC, PC + SWCNT, PP and PP + Ag MNPs in serum-free cell culture medium. Since particles tended to float in submerged conditions and since particle nebulisation did not yield reproducible results, a quasi-ALI approach was used for exposure. The exposure in quasi-ALI conditions is based on dispersing the MNPs w/ and w/o nanoparticles in culture medium and exposing the cells to 20 µL of each dispersion at different concentrations. The exposure concentrations 17.86 and 8.93 µg/cm^2 were chosen for both Calu-3 and MucilAir™ experiments. A higher concentration (31.25 µg/cm^2 sublethal concentrations based on cell viability test) was chosen only for the Calu-3 experiment, which corresponds to the maximum deposited dose in submerged conditions in 96-well plates (100 µL exposure and 0.32 cm^2 surface area). A serum-free medium only condition was used as negative controls and cells treated with 20 µL of 500 µg/mL lipopolysaccharides (LPS, Sigma Aldrich L4391) and 500 µL of 2% Triton X-100 were used as positive controls respectively for inflammation and cell viability (LDH).

2.4.3. *MucilAir model*

As with the Calu-3 exposure, MucilAir™ was exposed under quasi-ALI conditions, following the same procedure as stated in section 2.4.2, to various MNP concentrations—first to identify cytotoxic levels and then to assess sublethal responses at lower doses. Sublethal concentrations were selected based on a cell viability and barrier integrity experiments (Supplementary data), where cells were exposed for 24 h to 0.1 µg/mL (10^6 particles/cm^3, a realistic dose according to Rodríguez-Garraus et al. (2025), 10 µg/mL (10^8 particles/cm^3), 1000 µg/mL (10^{10} particles/cm^3) and 10,000 µg/mL (10^{11} particles/cm^3) (emissions from 3D printers previously reported in Azimi et al., 2016 and Stefaniak et al., 2019) of PC, PC + SWCNT, PP and PP + Ag MNPs. Briefly, as followed in Rodríguez-Garraus et al. (2025), emission of the particles was measured using the NanoScan SMPS Nanoparticle Sizer 3910 (TSI Incorporated) and Optical Particle Sizer (OPS) 3330 (TSI Incorporated) to establish the environmentally relevant concentration of the particles emitted. Untreated cells were used as negative controls and cells treated with 10% Triton X-100 were used as positive controls. For this preliminary experiment, 3 replicates per treatment and inserts coming from a single donor (male, age 42) were used. After exposures, cell viability (LDH) and cell barrier integrity (TEER) were evaluated, and results showed that 10,000 µg/mL significantly affect MucilAir viability and barrier integrity. Thus, 0.1 to 1000 µg/mL were selected for the subacute experiment.

The approach chosen for the subacute *in vitro* experiment was similar to the one described in the OECD TG 412 (Subacute Inhalation toxicity: 28-day study, 2018), using the advanced *in vitro* model MucilAir™ instead of rodents, to evaluate the robustness of the *in vitro* model. For this experiment, MucilAir™ inserts were exposed for 4 h/day (Monday to Friday, along 28 days) to 3 concentrations of PC, PC + SWCNT, PP and PP + Ag MNPs: 0.1, 10 and 1000 µg/mL. Cells were washed with 200 µL of PBS after the exposure time to remove the remaining particles and control the release of mucous and left in ALI conditions. Basolateral medium was collected at time 0, 4 h, 24 h, 7d, 14d, 21d and 28d, stored at −20 °C and renewed every 2 days. Reactivity of MNPs was measured using the FRAS assay. At time 0, 4 h, 24 h, 7d, 14d, 21d and 28d, cytotoxicity (LDH), barrier integrity (TEER) and cytokine release (Legendplex) were measured. At the end of the experiment (day 28),

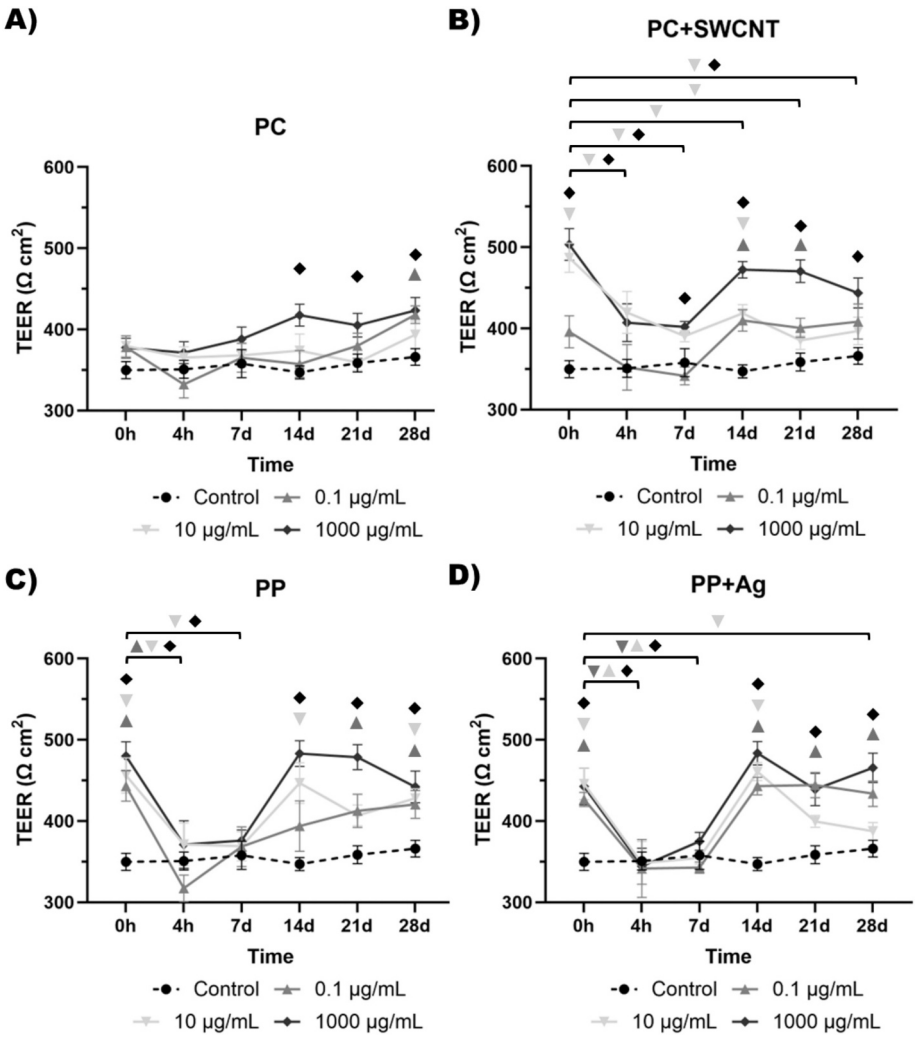

Fig. 8. Cell barrier integrity through transepithelial electric resistance (TEER) of MucilAir™ model exposed to 0.1, 10 and 1000 µg/mL of A) PC, B) PC + SWCNT, C) PP and D) PP + Ag MNPs for 4 h a day, 28 days. Results are expressed as TEER values ± SEM of 5 replicates per tested condition. $N = 3$. Symbols indicate significant differences with respect to the untreated control cells at the same timepoints ($p < 0.05$). Brackets indicate significant differences of each treatment with respect to t = 0 ($p < 0.05$).

oxidative potential (protein carbonylation), genotoxicity (Comet Assay) and cellular internalisation (TEM) were evaluated. For the subacute experiment, untreated cells were used as negative controls and cells treated with 0.1% Triton X-100, cytomix (1 µg/mL LPS + 0.1 µg/mL TNF-α + 1% FBS) and methyl methanesulfonate (MMS, 10 µg/mL) were used as positive controls respectively for cell viability/barrier integrity, inflammation and genotoxicity. Fig. 1 shows a schematic illustration of the exposures and endpoints evaluated at each exposure time.

2.5. Acute responses in Calu-3 cells

2.5.1. Cytotoxicity (LDH)

For the Calu-3 model, positive control inserts were exposed to 500 µL of 2% Triton X-100 for 10 min at room temperature on a shaker. Cytotoxicity was assessed by performing the Lactate Dehydrogenase (LDH) cytotoxicity assay according to the manufacturer's instructions (Cytotoxicity Detection Kit, Roche 11,644,793,001). After treatment of the model for 24 h, 100 µL of apical and basolateral supernatants were transferred to a new 96-well plate and 100 µL of LDH reagent was added. The positive control samples were diluted 10×. Samples were incubated for 20 min in dark at room temperature. After incubation, absorbance at 490 nm was measured. A range of LDH concentration (LDH standard, Roche Diagnostics 10,127,876,001) was include on the plate to allow for extrapolation of the absorbance to the concentration of LDH in µg/mL.

2.5.2. Cell barrier integrity by trans epithelial electrical resistance (TEER)

After the exposure of the model for 24 h, 500 µL of apical medium was added to the apical side of the inserts to facilitate the read-outs. Cell barrier integrity of Calu-3 model was evaluated by measuring the transepithelial electrical resistance (TEER) of the pulmonary barrier. Resistance was measured using an Epithelial Voltohmmeter (EVOM^2) coupled to a STX4 Electrode (EVOM™, World precision instruments, Sarasota, FL, USA). TEER readings were determined by subtracting the mean resistance of three inserts without cells (blank) from the recorded resistance of the pulmonary model and multiplying the obtained result by 1.12 (effective membrane surface area of the insert) to express the results in Ω·cm^2. After the TEER measurements, apical and basolateral media were collected, put on ice, centrifuged for 15 min at 10.000 x g at 4C to remove cell debris and particles, and either used for LDH assay immediately or stored at −80 for Legendplex analysis.

2.5.3. Inflammatory response - Legendplex

Cytokine secretion of Calu-3 cells after acute exposure was analysed using the Legendplex Human Essential Immune Response Panel (13-plex) (Biolegend, 740930), using an adapted reduced-volume screening protocol. Assay beads, antibodies and assay buffer were pre-mixed in a

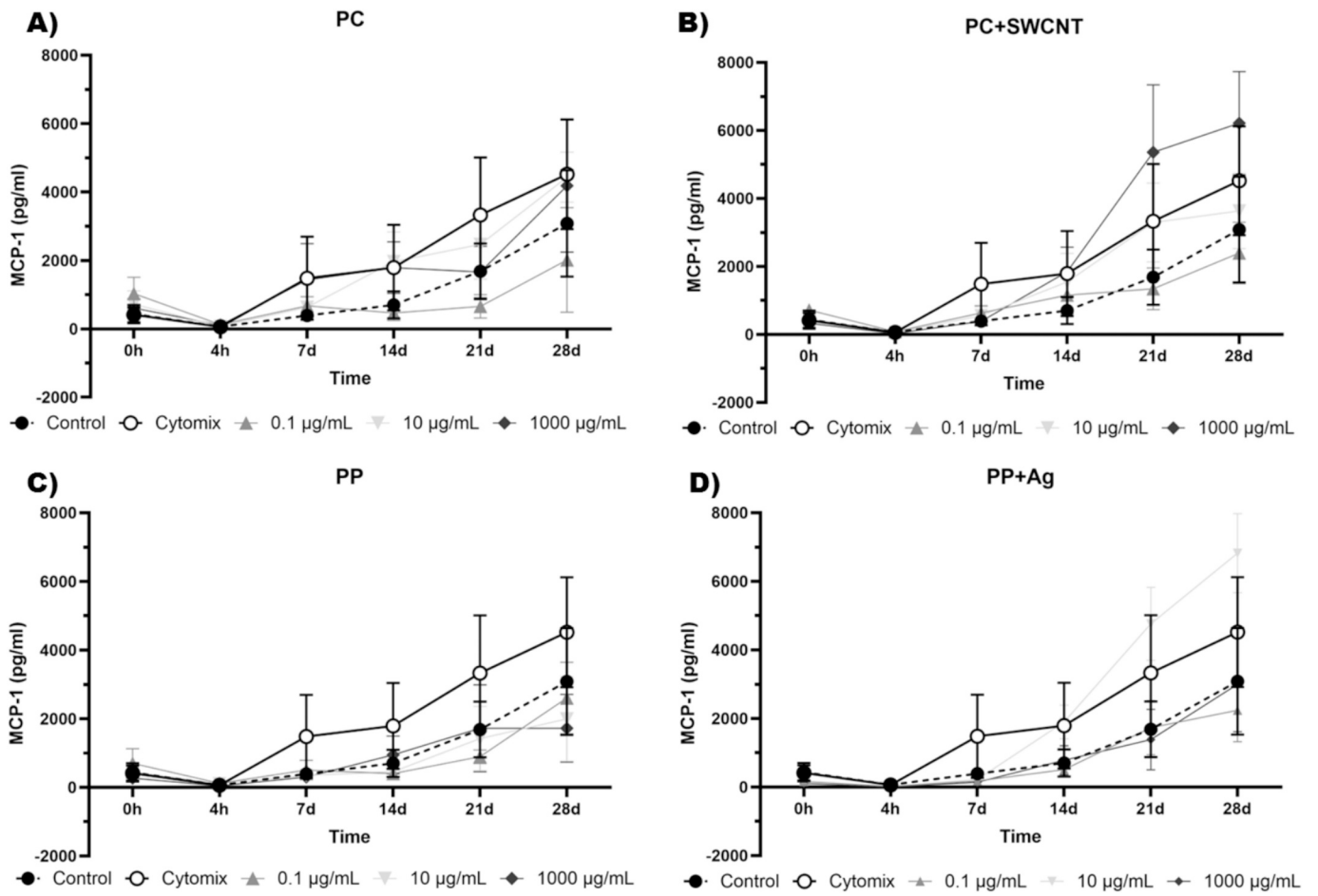

Fig. 9. MCP-1 release of MucilAir™ model exposed to 0.1, 10 and 1000 µg/mL of A) PC, B) PC + SWCNT, C) PP and D) PP + Ag MNPs for 4 h a day, 28 days. Results are expressed as mean value ± SEM of 5 replicates per tested condition. $N = 3$.

1:1:1 ratio, of which 15 µL was added to the wells of a Polypropylene V-bottom 96-wells plate (Falcon, 353263). Next, 5 µL of standards and samples collected from the apical and basolateral compartment after 24 h of exposure were added to the wells containing the bead-antibody mixture after pipetting the samples up and down to mix. Plates were incubated for 2 h at room temperature in the dark shaking at 600 rpm. After the incubations, 5 µL of Streptavidin phycoerythrin (SA-PE) was added to each well, after which the plates were incubated another 30 min at room temperature in the dark shaking at 600 rpm. Plates were washed by adding wash buffer and centrifugation for 5 min at 1000 xg, and beads were then resuspended in wash buffer.

Fluorescence was analysed using flow cytometry (BD FACSCanto) using settings previously optimized with the reference beads included in the Legendplex kit. PE and APC channels were used and 4000 events were analysed per well. Biolegend Qognit software was used for data analysis, and all gates were manually reviewed. The software automatically calculates cytokine concentrations based on the standard curves, and these were used in the manuscript. Supernatants from three experiments were analysed, with two technical replicates per experiment.

2.6. Acute responses in TK6 cells

2.6.1. Genotoxicity - micronucleus (MN) assay

TK6 cells were processed for the MN assay as described in Rodríguez-Garraus et al. (2023), except that no cell sorting beads were used. Instead, cell counting was performed, before the treatment and at the end of the culture, by staining the cells with 4.5 µg/mL of propidium iodide (ThermoFisher) and analysing the number of living cells using the CytExpert software (version 2.4; Beckman Coulter Inc., Brea, CA, USA). The same software was used for analysing the frequency of MN from a minimum of 20,000 nuclei per condition based on the Litron gating strategy (Litron Laboratories, Rochester, New York, USA).

The micronucleus (MN) assay was performed in TK6 cells based on the adapted OECD TG 487 for testing of nanomaterials (OECD, 2022; Burgum et al., 2024) in combination with the flow cytometry-based scoring method (Franz et al., 2020). As required by the OECD TG 487, cytotoxicity was determined in the same experiment as the induction of MN. For each test condition, the relative increase in cell counts (RICC) was calculated as described at the test guideline. Only concentrations showing a RICC above 45 ± 5%, equivalent to 55 ± 5% cytotoxicity, were considered for the analyses of MN.

2.7. Acute and subacute responses in MucilAir™

2.7.1. Cytotoxicity (LDH)

Cytotoxicity was assessed by performing the LDH cytotoxicity assay according to manufacturer' instructions (CytoTox 96® Non-Radioactive Cytotoxicity Assay, Promega G1780). Briefly, 50 µL of the basal medium was collected at 0 and 4 h and days 7, 14, 21 and 28, and incubated with 50 µL of CytoTox 96® Reagent for 30 min at room temperature protected from light. After the incubation time, 50 µL of the Stop Solution was added to each sample and the absorbance was measured at 490 nm. Cytotoxicity was expressed as percentage of LDH released in treated cells respect to the release of untreated control cells. Inserts treated with 0.1% Triton X-100 were used as positive control.

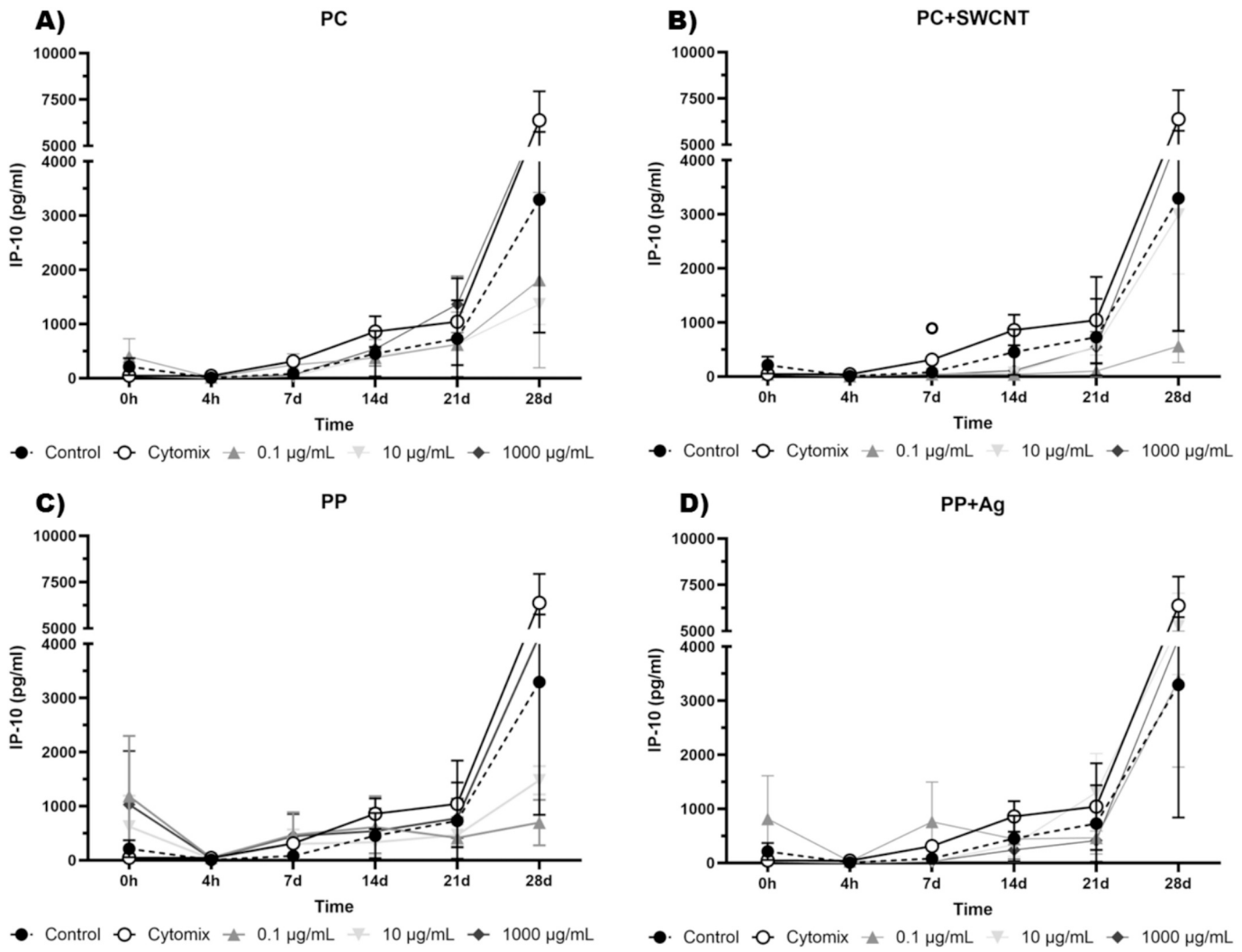

Fig. 10. IP-10 release of MucilAir™ model exposed to 0.1, 10 and 1000 µg/mL of A) PC, B) PC + SWCNT, C) PP and D) PP + Ag MNPs for 4 h a day, 28 days. Results are expressed as mean value ± SEM of 5 replicates per tested condition. N = 3.

2.7.2. Cell barrier integrity by trans epithelial electrical resistance (TEER)

Cell barrier integrity of the model was evaluated by measuring the transepithelial electrical resistance (TEER) of the pulmonary barrier. Resistance was measured using an Epithelial Voltohmmeter (EVOM^2) coupled to a STX4 Electrode (EVOM™, World precision instruments, Sarasota, FL, USA). TEER readings were determined by subtracting the mean resistance of three inserts without cells (blank) from the recorded resistance of the pulmonary epithelium and multiplying the obtained result by 0.33 (effective membrane surface area of the insert) to express the results in Ω·cm^2. Before TEER measurements, culture medium from basal chamber was either removed or collected and a saline solution (Modified Hanks' Balanced Salts without calcium chloride, magnesium sulphate and phenol red, H4891 Sigma-Aldrich) was added both in apical and basal chambers. After TEER readings, the saline solution was discarded, and fresh culture medium was replaced in the basal chamber.

2.7.3. Inflammatory response - Legendplex

Cytokine secretion from MucilAir™ was carried out according to the protocol described in Section 2.5.3. Cytokine secretion was quantified using basolateral samples collected at 0 and 4 h, and at days 7, 14, 21, and 28.

2.7.4. Genotoxicity – Comet assay

Due to lack of cell division in the MucilAir model, which is a requirement for the micronucleus assay, genotoxicity was evaluated using the Comet assay instead, following Jackson et al. (2013). Briefly, after 28 days of exposure, cells were washed with PBS and detached from the inserts. Cells were then washed twice by centrifuging cell suspensions (300 g, 5 min) in PBS. The resulting cell suspensions were centrifuged (300 g, 5 min) and resuspended in cell culture medium with 10% DMSO and frozen at −80 °C.

Processing of samples was performed based on a previously published protocol (Jackson et al., 2013) where cells were thawed quickly and 50 µL of the cell suspension was embedded in 200 µL of molten (37 °C) 1% low-melting-point agarose (Merck, Darmstadt, Germany). As internal positive control, cells from unexposed inserts were treated with 20 mM H_2O_2 (Riedel-deHaen, Seelze, Germany) for 10 min before being embedded in agarose. Two 40 µL drops (approx. 20,000 cells/drop) of the resuspended cells were pipetted onto dry microscope slides precoated with 1.5% normal-melting-point agarose (Electran 443666 A, VWR International, Leuven, Belgium), and the agarose was allowed to solidify for 10 min. The slides were then immersed in cold lysing solution (2.5 M NaCl, 100 mM EDTA, 10 mM Tris, 10% DMSO, 1% Triton X-100) at 4 °C and left overnight.

The following day, an electrophoresis was performed with the sample slides for 20 min at 0.67 V/cm and 300 mA. The slides were then neutralized with cold PBS washes and cold distilled water, fixed in 96% EtOH (Berner, Helsinki, Finland) for 5 min, air-dried and store at room

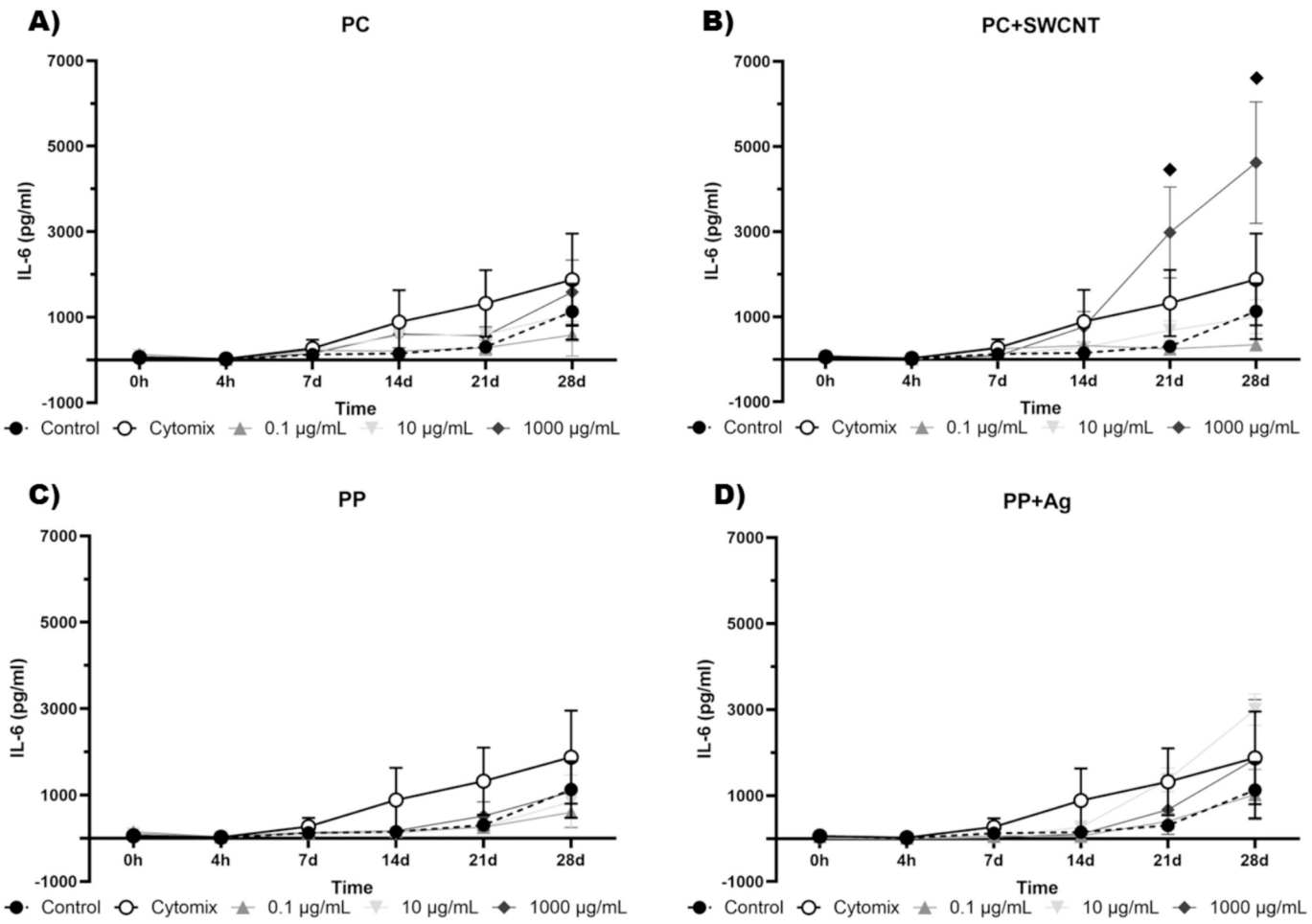

Fig. 11. IL-6 release of MucilAir™ model exposed to 0.1, 10 and 1000 µg/mL of A) PC, B) PC + SWCNT, C) PP and D) PP + Ag MNPs for 4 h a day, 28 days. Results are expressed as mean value ± SEM of 5 replicates per tested condition. N = 3. Symbols indicate significant differences with respect to the untreated control cells at the same timepoints ($p < 0.05$).

temperature until being stained. For staining, 2 µg/mL ethidium bromide (WR Chemicals, Solon, USA) was used to analyse the slides by fluorescence microscopy (Axioplan 2, Zeiss, Jena, Germany) and interactive automated comet counting (Komet 7.1, Andor an Oxford Instruments company, Belfast, UK). A total of 200 cells per treatment and experiment (two replicates per concentration, two gels per replicate, 50 cells/gel) were scored and the results were calculated as mean percentage of DNA in the comet tail.

2.7.5. *Internalisation*

Rodríguez-Garraus et al. (2025), already confirmed that both PC and PP MNPs internalise equally into cells. Thus, to confirm that MNPs were internalized in the cells, TEM analysis was performed only with PC. Briefly, after 28-day exposure, cells were washed with 0.2 M PHEM buffer (PIPES 60 Mm, HEPES 25 mM, 10 Mm $MgCl_2$, 2 mM EGTA, pH 7) twice to remove the remaining particles. Afterwards, the inserts were first fixed with 4% PFA/0.4% GA (in PHEM 0.1 M) for 30 min at room temperature, followed by a second fixation with 2% PFA/0.2% GA (in PHEM 0.1 M) for 30 min at room temperature. Once cells were fixed, inserts were washed 3 times with 0.1 M PHEM buffer and placed in PHEM buffer at 4 °C overnight. Samples were then dehydrated using increasing concentrations of ethanol (30%, 50%, 70%, 90%, 96%, 100%, 100%), submerging the samples for 10 min in each ethanol concentration. Afterwards, samples were immersed in Epoxy resin and polymerized to create a solid block. Finally, samples were sectioned using an ultramicrotome to cut ultra-thin sections and mount them on TEM grids.

2.7.6. *Oxidative potential - protein Carbonylation*

The protein carbonylated content was determined by using an ELISA kit for protein carbonyl detection (ab238536, Abcam). MucilAir™ cultures were treated at three different concentrations of each one of the materials (0.1, 10 and 1000 µg/mL), maintained in culture for 28 days, when cells were washed in PBS and preserved at −80 °C until further use. Cell lysates were obtained by lifting and collecting cells in 150 µL of PBS per well, sonicating using a tip sonicator for 10 s 2 times, and centrifugating at 10000 x g for 20 min to remove cellular debris. 100 µL of 10 µg/mL protein samples were first allowed to adsorb to wells of a 96-well plate and then react with dinitrophenylhydrazine (DNPH), which allows for derivatization of the carbonyl group. The quantity of protein carbonyls in protein sample was then determined by comparing its absorbance with that of a known reduced/oxidized BSA standard curve. Results are expressed as percentage of the negative control consisting of non-treated cultures.

2.8. *Statistical analysis*

In all assays, data are presented as mean value ± standard error (SE). Normality of the data was verified through the Kolmogorov–Smirnoff test and the homogeneity of the variances through the Levene's test. Differences among groups were assessed by Kruskal-Wallis test followed by a Dunn post-hoc test. A p-value ≤ 0.05 was considered statistically significant. All analysis were performed using the GraphPad Prism 10.1.0 statistic software.

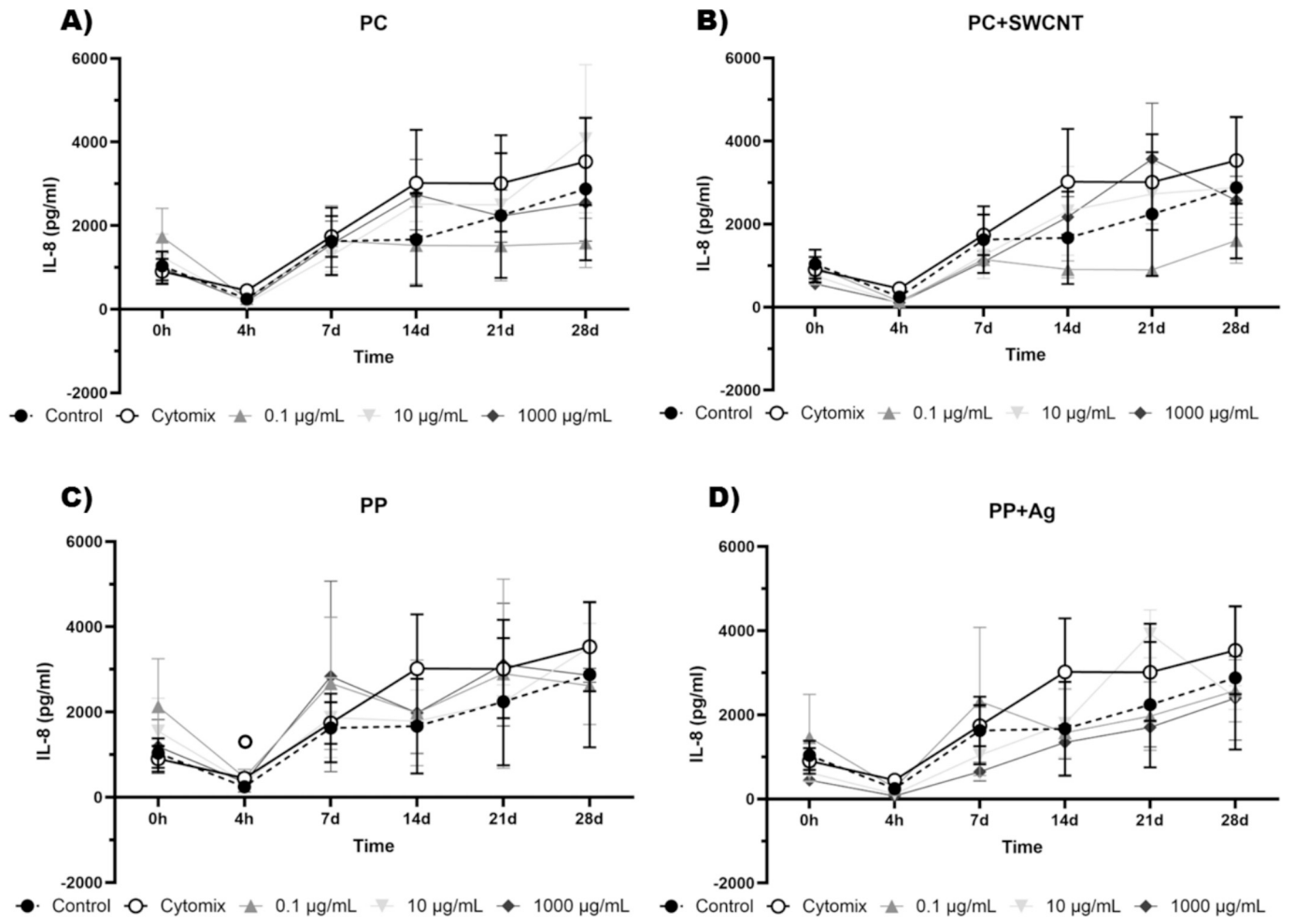

Fig. 12. IL-8 release of MucilAir™ model exposed to 0.1, 10 and 1000 µg/mL of A) PC, B) PC + SWCNT, C) PP and D) PP + Ag MNPs for 4 h a day, 28 days. Results are expressed as mean value ± SEM of 5 replicates per tested condition. N = 3.

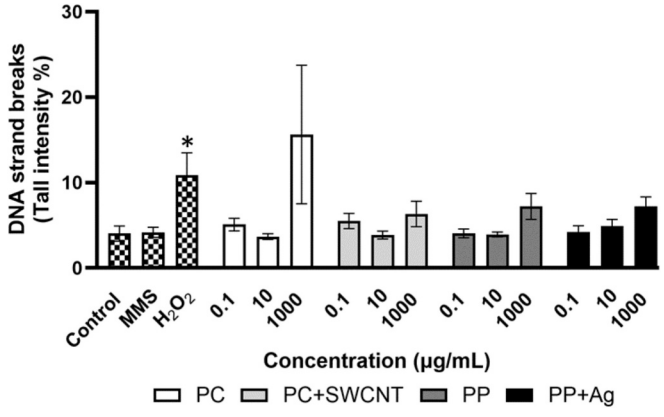

Fig. 13. Genotoxic damage of MucilAir™ model exposed to 0.1, 10 and 1000 µg/mL of PC, PC + SWCNT, PP and PP + Ag MNPs for 4 h a day, 28 days. Results are expressed as mean value ± SEM of 2 replicates per tested condition. $N = 2$. Symbols indicate significant differences with respect to the untreated control cells ($p < 0.05$). Positive control Methyl methanesulfonate (MMS) was used at 10 µg/mL. H_2O_2 at 20 mM was used as internal control for Comet assay.

3. Results

3.1. Characterization and reactivity of the MNPs

Characterization of MNPs is fully reported in Rodríguez-Garraus et al. (2025). Briefly, all samples contained a few particles >1 µm (1–13%), and the majority varying from 0.25 to 0.30 µm. ICP-MS analysis showed 0.052 wt% of Ag NPs in the PP + Ag sample, whereas Raman analysis showed that PC + SWCNTs sample contained 0.425 wt% SWCNT. Results from DLS measurements and PDI, reported in Rodríguez-Garraus et al. (2025), showed no significant differences among the MNPs in both dispersants. However, size measurements showed high variability, as expected in DLS measurements of highly polydisperse fractions of MNPs (Domenech et al., 2024; Rodríguez-Garraus et al., 2025). On the other hand, all particles had negatively charged surfaces in both dispersants, with a *Z*-potential of −3.76 to −11.13 mV, indicating low stability of the MNP suspensions (Rodríguez-Garraus et al., 2025).

As part of the reactivity characterization, oxidative potential was measured using the FRAS assay. Results obtained (Fig. 2) showed low oxidative potential for all the MNPs tested, as none of the materials exceeded 10% of the CuO positive control for any of the concentrations tested, therefore, results for MNPs were classified as low potential for oxidative damage (< 10% BOD).

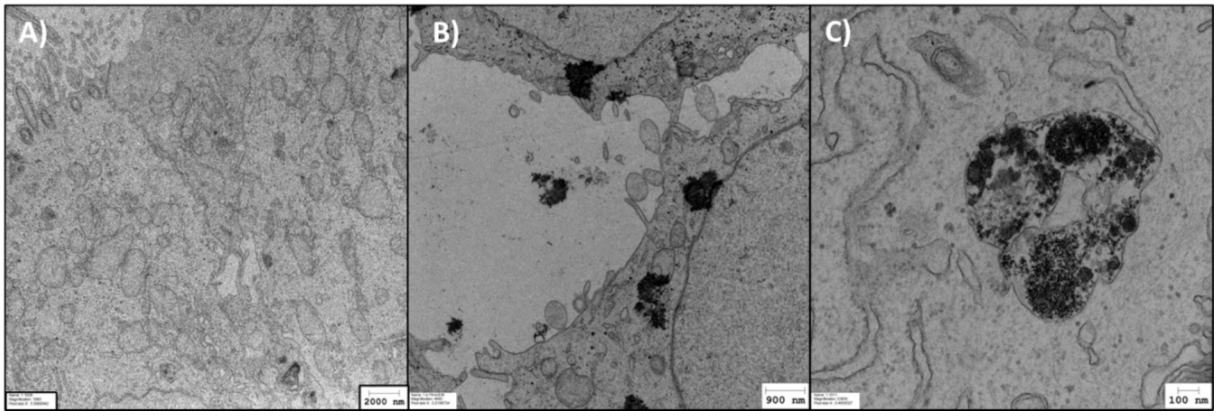

Fig. 14. TEM analysis of MucilAir™ model exposed to 10 μg/mL for 28 days. A) Normal cell morphology, B) and C) PC MNPs. Scale bars show the magnification of the images.

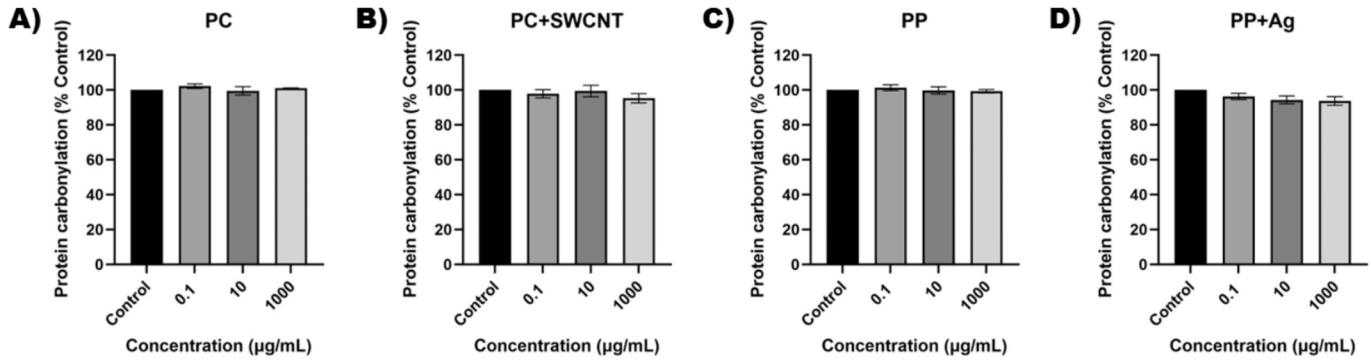

Fig. 15. Oxidative damage (Protein carbonylation) of MucilAir™ model exposed to 0.1, 10 and 1000 μg/mL of A) PC, B) PC + SWCNT, C) PP and D) PP + Ag MNPs for 4 h a day, 28 days. Results are expressed as mean value ± SEM of 2 replicates per tested condition. N = 3. No significant differences were observed.

3.2. Acute responses in Calu-3 cells

3.2.1. Cytotoxicity (LDH)

Based on the cytotoxicity results of Calu-3 model, exposure to MNPs with and without NMs for 24 h induced no significant cytotoxic effects by means of LDH release (Fig. 3) for any of the concentrations tested.

3.2.2. Cell barrier integrity by trans epithelial electrical resistance (TEER)

Based on TEER results of Calu-3 model, exposure to MNPs with and without NMs for 24 h induced no significant changes in the integrity of the pulmonary barrier (Fig. 4) for any of the concentrations tested.

3.2.3. Inflammatory response - Legendplex

Release of MCP-1, IP-10, IL-6 and IL-8 pro-inflammatory cytokines and chemokines were analysed. Based on the results of Calu-3 model, exposure to MNPs with and without NMs for 24 h induced no significant release of any of these cytokines (Fig. 5) for any of the concentrations tested. A significant increase of IL-6 and IL-8 was detected only after exposures to LPS (Fig. 5 C and D).

3.3. Acute responses in TK6 cells

3.3.1. Genotoxicity – Micronuclei (MN) assay

Genotoxicity effects were assessed following the adapted OECD TG 487 (Burgum et al., 2024) for nano-sized materials in TK6 cells. RICC results (Fig. 6) showed a significant cytotoxic effect of PC, PP and PP + Ag MNPs starting at 50 μg/mL and PC + SWCNT starting at 25 μg/mL. Based on the criteria of the OECD TG 487, only concentrations showing RICC below 45 ± 5% (equivalent to 55 ± 5% cytotoxicity) were considered for MN analysis, as at higher cytotoxic levels, unspecific genotoxic effects may appear due to a general downfall of cellular functions. Based on the results obtained from the MN assay (Fig. 6), none of the MNPs induced the generation of MN for any of the concentrations considered.

3.4. Acute to sub-acute responses in MucilAir™

3.4.1. Cytotoxicity (LDH)

A baseline of 5% of LDH release is considered normal in healthy MucilAir™ tissue, based on the data provided by manufacturers. Based on the cytotoxicity results, exposure to MNPs with and without NMs for 28 days induced an increase in cytotoxicity by means of LDH release (Fig. 7). Short-term exposure (<7 days) to MNPs with and without NMs did not significantly affect the viability of cells, however after 7 days of exposure, LDH release significantly increased in cells treated with 0.1 and 10 μg/mL of PC (Fig. 7 A). At day 14, LDH release was significantly higher compared to untreated cells after the exposure to 10 μg/mL of PC and PC + SWCNT MNPs (Fig. 7 A and B). PC showed higher cytotoxicity than PC + SWCNT, starting at day 7 of exposure and being significantly higher than the negative control at day 21 for 10 and 1000 μg/mL, whereas PC + SWCNT was only significantly cytotoxic for 10 μg/mL at day 21 (Fig. 7 A and B). On the other hand, LDH release significantly increased at days 21 and 28 after the exposure to 10 and 1000 μg/mL of PP + Ag (Fig. 7 D), while this effect was only significant at day 28 after the exposure to 0.1 and 1000 μg/mL of PP (Fig. 7 C), indicating a higher cytotoxicity of PP + Ag in contrast to PP alone.

3.4.2. Cell barrier integrity by trans epithelial electrical resistance (TEER)

According to the commercial supplier MucilAir™ TEER values of healthy tissue should be higher than 200 Ω cm^2. Results showed a

significant increase of TEER after the exposure to 1000 μg/mL of PC, PC + SWCNT, PP and PP + Ag MNPs in contrast to untreated control after day 14 (Fig. 8). In addition, PC + SWCNT also induced an increase of TEER values at days 14 and 21 after the exposure to 0.1 and 10 μg/mL and only 0.1 μg/mL, respectively (Fig. 8 B). PC + SWCNT showed a more remarkable effect in TEER values in contrast to PC after 14 days of exposure. In addition, both PP and PP + Ag MNPs significantly affected TEER values after day 14 of exposure in contrast to untreated cells (Fig. 8 C and D). Moreover, significant differences were observed for every timepoint after the exposure of MucilAir model to 10 μg/mL PC + SWCNT, as well as 1000 μg/mL at 4 h, 7 and 28 days (Fig. 8 B), in comparison to $t = 0$. Significant differences were also observed in 10 and 1000 μg/mL PP at 4 h and 7 days and 0.1 μg/mL PP at 4 h (Fig. 8 C), as well as all the concentrations of PP + Ag at 4 h and 7 days, and 10 μg/mL PP + Ag at 14 days (Fig. 8 D) in contrast to t = 0.

3.4.3. *Inflammatory response - Legendplex*

MCP-1 displayed a non-significant tendency to increase following 28-day exposure to MNPs, both with and without NMs. Nevertheless, an upward trend in MCP-1 release became apparent after day 7 (Fig. 9), particularly for 1000 μg/mL PC + SWCNT and 10 μg/mL PP + Ag.

Similarly, IP-10 showed a non-significant increase after 28 days of exposure to MNPs with and without NMs. However, a rising tendency in IP-10 release was observed at days 21 and 28 (Fig. 10).

IL-6 showed a tendency to increase inflammation after 7 days exposure and a significant release after the exposure to 1000 μg/mL of PC + SWNCT at days 21 and 28 (Fig. 11 B).

IL-8 showed a non-significant increase after 7 days of exposure to MNPs with and without NMs. (Fig. 12).

3.4.4. *Genotoxicity – Comet assay*

Based on the results obtained from the Comet assay, no significant genotoxic effects were observed after the exposure of MucilAir™ model to MNPs with and without NMs for 28 days in contrast to negative control (Fig. 13). However, a slight but not significant effect could be observed for the highest concentration of the MNPs, specially, for 1000 μg/mL PC.

3.4.5. *Internalisation*

As already described in Rodríguez-Garraus et al. (2025), both PP and PC MNPs internalise equally into the cells. Thus, a fast screening using PC was performed to confirm the internalisation of MNPs into the cells after 28 days of exposure to 10 μg/mL of PC. Results obtained from TEM analysis indicated that PC particles were effectively internalized inside the cells (Fig. 14), suggesting that the particles might accumulate in the lysosomes.

3.4.6. *Oxidative potential – Protein carbonylation*

Formation of protein carbonyls is highly useful for studying oxidative stress as it is the most prevalent type of irreversible protein oxidation that can be promoted by intracelular ROS. The content of carbonylated proteins was assessed in lysates of MucilAir™ cultures treated for 28 days at three different concentrations of each one of the materials (0.1, 10 and 1000 μg/mL), None of the materials at the concentrations tested showed significant differences when compared to the negative control (Fig. 15). Therefore PC, PC + SWCNTs, PP and PP + Ag do not increase protein carbonylation in MucilAir™. These results are in line with the low oxidative potential observed for the materials in the FRAS assay (Fig. 2).

4. Discusion

3D printing has advanced in several applications, and new formulations combining polymers with nanomaterials have been used to enhance their properties. Mechanical recycling of 3D-printed plastic polymers can generate secondary particles, including micro- and nanoplastics (MNPs). As the use of these materials expands, the mechanical breakdown of plastics during recycling of 3D printed materials may elevate human exposure to MNPs, prompting concerns about potential health risks for users and broader environmental impacts. In addition to the recycling process, during the 3D printing of PC, PC + SWCNT, PP, and PP + Ag materials, MNPs are released. Rodríguez-Garraus et al. (2025) collected and quantified emitted MNPs and found that the amounts released in a workplace setting were comparable to the lowest concentration tested in this study, supporting the relevance of the concentrations used.

For *in vitro* particle exposure, the initial strategy involved nebulising the particles using a commercial device, such as the Vitrocell Cloud System, which enables simulation of inhalation exposure. (Meindl et al., 2023). However, this approach proved impractical because the MNPs displayed widely differing sedimentation rates and highly variable particle sizes (1–13 μm), which prevented achieving a uniform exposure (data not shown). Therefore, a quasi-ALI exposure was chosen, in which the model was exposed to a thin 20-μL liquid MNP suspension layer that was quickly absorbed, promoting direct contact between the MNPs and the cells (Cervena et al., 2019; Meindl et al., 2023; Welch et al., 2021).

Results from acute exposures of Calu-3 cells to PC and PP MNPs, alone or in combination with SWCNT and Ag respectively, showed that MNPs did not cause significant cytotoxicity at any tested concentrations. Similar results were observed in Meindl et al., 2023, where acute exposure of Calu-3 did not lead to significant decrease in cell viability. This may be due to the fact that Calu-3 cells produce mucus, which acts as a protective barrier (Meindl et al., 2023; Welch et al., 2021). Similarly, acute exposures of MucilAir™ to these MNPs did not cause cytotoxicity, however, subacute repeated exposures (starting from day 7) caused significant increase of LDH release. After 7 days, LDH levels showed a slight stabilisation, and only some concentrations continued to induce significant damage compared with untreated cells. A similar trend has been reported in previous studies examining the effects of polycyclic aromatic compounds or carbon nanotubes on MucilAir model along 28 days of exposure (Cervena et al., 2019; Meindl et al., 2023; Welch et al., 2021). The results indicate a potential for lung tissue recovery, possibly reflecting cellular adaptation to the damage (Crespin et al., 2014). This adaptation may occur through the regeneration of damaged areas, where undamaged progenitor cells migrate, proliferate, and differentiate to regenerate the epithelium. Thus, the cells may be able to partially counteract or repair the damage induced by these compounds (Kooter et al., 2017; Welch et al., 2021). However, based on our findings, prolonged exposures ultimately result in increased LDH release, likely because the cells can restore only basic functions and are unable to achieve full recovery (Welch et al., 2021).

The assessment of TEER (Transepithelial Electrical Resistance) is a widely used quantitative technique to measure the integrity of tight junctions in endothelial and epithelial barrier models without causing cellular damage (Srinivasan et al., 2015). TEER results obtained from Calu-3 cells showed values above 300 $\Omega \cdot cm^2$, which are higher than previously reported standards (Meindl et al., 2023; Ren et al., 2012), indicating proper formation of the pulmonary barrier. According to the results, exposing the Calu-3 model to secondary MNPs from 3D printing waste did not affect TEER values, suggesting that no significant damage occurred to the pulmonary barrier. This could be due, in line with the cytotoxicity results, to protection by the mucus barrier, which may prevent the particles from damaging the cell layer (Meindl et al., 2023; Welch et al., 2021). On the other hand, the MucilAir model also showed TEER values above 200 $\Omega \cdot cm^2$, which indicates healthy lung tissue (Rossner et al., 2019), according to the threshold values provided by Epithelix. The results obtained after subacute exposure of the MucilAir model showed a significant loss of barrier integrity after 4 h and 7 days of exposure to the MNPs. However, TEER values recovered after day 14, which could be due to a cellular damage adaptation mechanism, as previously mentioned. Previous studies (Cervena et al., 2019; Haswell et al., 2021; Welch et al., 2021) showed a similar trend, where MucilAir

TEER values decreased after 5–7 days of exposure followed by recovery. If the damage is not irreversible, this adaptation mechanism allows the repopulation of damaged areas, enabling the formation of new tight junctions (Welch et al., 2021). Finally, the significant increase in barrier integrity after 7 days of exposure could be due to accumulation of MNPs in the mucus layer (Meindl et al., 2023), leading to increased transepithelial resistance and, consequently, higher TEER values (Welch et al., 2021).

Regarding inflammation, acute exposure of Calu-3 cells to MNPs did not significantly trigger the production of any of the inflammatory markers analysed. However, exposure to PP resulted in a slight increase in all four inflammatory markers. A similar effect was seen in MucilAir™, where the inflammatory response showed a slight increase but was not significantly induced. Up to day 7 of exposure, this low level of inflammation may indicate minimal damage to the lung tissue—either due to a balanced response between the pro-inflammatory and anti-inflammatory cytokines (Meindl et al., 2023), or because of protection conferred by the mucus layer (Rossner et al., 2021). However, after day 7, an accumulation of these inflammatory markers was observed, suggesting cellular damage (Meindl et al., 2023; Rossner et al., 2021). These results are corroborated with previous findings (Meindl et al., 2023), where a rising trend in IL-6 and IL-8 was observed during 7–14 days of exposure, although this effect later was counteracted. A low inflammatory response could also be due to the presence of the mucus barrier (Metz et al., 2018). In relation with the rise in LDH release, only a slight increase in IL-6 and IL-8 was observed, possibly due to a higher proportion of damaged cells, which may have contributed to greater variability in the results. (Kooter et al., 2017). Additionally, donor variability is a critical factor contributing to differences in inflammatory marker release (Kooter et al., 2017; Rossner et al., 2021). Alternative assays, such as RNA expression analysis, could be considered as less variable parameters to evaluate the potential effects of MNPs from recycling of 3D printing waste on inflammatory marker expression (Kooter et al., 2017).

Oxidative damage is a key factor in assessing the potential toxicity of chemicals and materials, as it reflects their capacity to generate reactive oxygen species (ROS). Acellular *in vitro* assays, such as the FRAS assay, are commonly used to assess the oxidative potential of materials. In contrast, cellular assays, like protein carbonylation, offer both qualitative and quantitative information on the oxidative damage experienced by cells. Carbonylated proteins lose their functionality within cellular systems and accumulate, potentially forming large aggregates that contribute to cellular dysfunction. As observed in the FRAS assay, the MNPs exhibited low oxidative potential, as did the materials with added NMs, indicating that the addition of NMs such as SWCNT or Ag does not enhance the oxidative potential of PC and PP, respectively. Additionally, although TEM imaging, and further detailed analysis in Rodríguez-Garraus et al. (2025) confirmed the internalisation of MNPs, no effects were observed on protein carbonylation. This suggests that the particles themselves do not induce oxidative damage and do not trigger intracellular REDOX reactions. (Kohl et al., 2020).

Genotoxicity may be caused by direct interaction of the material with the genetic material of the cell, but it requires a direct physical contact of the material with the DNA (Kohl et al., 2020), which may lead to DNA strand break or interfere with the process of mitosis, leading to formation of micronuclei (Kisin et al., 2011). However, indirect genotoxic effects may also be induced by oxidative damage (Kohl et al., 2020; Rodríguez-Garraus et al., 2023). In fact, the induction of oxidative stress as a result of exposure to nanomaterials may lead to inflammatory responses and oxidative/genotoxic damage (Ruijter et al., 2024). Based on the results in TK6 model, no significant formation of micronuclei was observed. In fact, a dose-dependent decrease in micronuclei formation was detected. This effect may be related to the increased LDH release observed in the MucilAir model, reflecting cells undergoing necrosis or apoptosis, or it could result from reduced interaction between the cells and MNPs, as particle aggregation may limit cellular contact (Burgum et al., 2024; Rodríguez-Garraus et al., 2023). In the MucilAir™ no significant DNA strand breaks were observed after 28 days of exposure to the MNPs. This lack of DNA breakage could result from low interaction of the particles with cellular genetic material (Rodríguez-Garraus et al., 2023) or DNA repairing mechanisms (Kohl et al., 2020). Considering that genotoxicity can be induced by oxidative stress and MNPs showed low oxidative potential, this could also support the observations made with genotoxicity effects (Kohl et al., 2020). In addition, these materials were used to assess the cell-transforming potential in Bhas-42 cell line, and results showed that these MNPs derived from 3D printing waste did not induce any cell-transforming effects either for tumour initiation or tumour promotion (Rodríguez-Garraus et al., 2025), suggesting the lack of genotoxic effects of these particles.

Some variability in the results from MucilAir™ was particularly notable, with the inflammatory response showing especially high fluctuations. This variability may be attributed to the use of cells from different donors (Rossner et al., 2021). Despite this, the MucilAir™ model demonstrates strong robustness for long-term exposures, while also showing sensitivity to cell viability and inflammation over time.

5. Conclusions

Overall, acute *in vitro* exposures of TK6 and Calu-3 cells and acute and subacute exposures of MucilAir™ showed different sensitivity and robustness. The TK6 model, a straightforward immune model used for adapting OECD TG 487 to nanomaterial testing, showed no significant genotoxic effects from secondary MNPs generated during the lifecycle of wasted plastic materials produced by 3D printing. However, exposure to the positive control (MMC) produced high genotoxicity, confirming the validity of the assay and indicating that the MNPs themselves were not genotoxic. On the other hand, Calu-3 model is a simple and easy-to-use model of the epithelial bronchial barrier. In the present study, MNPs did not caused remarkable toxic effects on Calu-3 cells. MucilAir™ showed greater sensitivity and robustness after acute and subacute exposures to MNPs, indicating that these particles induce cytotoxic and inflammatory effects, that could be prolonged over time, potentially affecting the integrity of the human *in vitro* respiratory system. Overall, acute exposure of MNPs with and without NM additives do not induce significant effects in the human pulmonary system, however, a long-term exposure to these particles might constitute a health risk. Lastly, our study provides insight into the potential of using an *in vitro* model in place of *in vivo* approaches by adapting OECD TG 412. This suggests that NAMs could serve as strong alternatives to animal testing and, in the future, may even replace animal models altogether.

CRediT authorship contribution statement

Itziar Polanco-Garriz: Writing – review & editing, Writing – original draft, Visualization, Methodology, Investigation, Formal analysis, Conceptualization. **Juliana Carrillo-Romero:** Methodology, Investigation. **Mari Venäläinen:** Writing – review & editing, Methodology, Investigation, Formal analysis, Conceptualization. **Jussi Lyyränen:** Writing – review & editing, Investigation. **Hanna Pulli:** Writing – review & editing, Investigation. **Satu Suhonen:** Writing – review & editing, Investigation. **Jolanda Vermeulen:** Investigation, Formal analysis. **Nienke Ruijter:** Writing – review & editing, Methodology, Investigation, Formal analysis, Conceptualization. **Ana Candalija Iserte:** Writing – review & editing, Methodology, Investigation, Formal analysis, Conceptualization. **Apostolos Salmatonidis:** Resources, Methodology, Conceptualization. **Marie Carriere:** Methodology, Conceptualization. **Morgan Lofty:** Resources, Methodology, Conceptualization. **Matthew Boyles:** Writing – review & editing, Methodology, Conceptualization. **Davide Lotti:** Resources. **Jesús C. Guzmán-Mínguez:** Resources. **José F. Fernández:** Resources. **Flemming Cassee:** Methodology, Conceptualization. **Julia Catalán:** Writing – review & editing, Methodology, Conceptualization. **Isabel Rodríguez-Llopis:** Writing – review &

editing, Methodology, Conceptualization. **Socorro Vázquez-Campos:** Visualization, Supervision, Project administration, Conceptualization. **Felipe Goñi de Cerio:** Project administration, Methodology. **Alberto Katsumiti:** Project administration, Methodology.

Declaration of competing interest

The authors declare that they have no known competing financial interests or personal relationships that could have appeared to influence the work reported in this paper.

Acknowledgements

This study was carried out and funded by the EU H2020 Project "Simple, robust and cost-effective approaches to guide industry in the development of safer nanomaterials and nano-enabled products (SAbyNA) under Grant Agreement no. 862419. Special thanks to EU Horizon Project "Safe and Sustainable by Design Advanced Materials" (SUNRISE) under Grant Agreement no. 101137324 for supporting this work.

Appendix A. Supplementary data

Supplementary data to this article can be found online at https://doi.org/10.1016/j.impact.2026.100631.

Data availability

Data will be made available on request.

References

Arrizubieta, J.I., Ukar, O., Ostolaza, M., Mugica, A., 2020. Study of the environmental implications of using metal powder in additive manufacturing and its handling. Metals 10 (2), 261. https://doi.org/10.3390/MET10020261.

Azimi, P., Zhao, D., Pouzet, C., Crain, N.E., Stephens, B., 2016. Emissions of ultrafine particles and volatile organic compounds from commercially available desktop three-dimensional printers with multiple filaments. Environ. Sci. Tech. 50 (3), 1260–1268. https://doi.org/10.1021/ACS.EST.5B04983.

Becker, R.C., Sadayappan, S., 2020. Designing human in vitro models for drug development. J. Am. Coll. Cardiol. 75 (6), 587–589. https://doi.org/10.1016/J.JACC.2019.12.013.

Burgum, M.J., Ulrich, C., Partosa, N., Evans, S.J., Gomes, C., Seiffert, S.B., Landsiedel, R., Honarvar, N., Doak, S.H., 2024. Adapting the in vitro micronucleus assay (OECD Test Guideline No. 487) for testing of manufactured nanomaterials: recommendations for best practices. Mutagenesis 39 (3), 205–217. https://doi.org/10.1093/MUTAGE/GEAE010.

Casati, S., 2018. Integrated approaches to testing and assessment. Basic Clin. Paharmacol. Toxicol. 123, 51–55. https://doi.org/10.1111/bcpt.13018.

Cervena, T., Vrbova, K., Rossnerova, A., Topinka, J., Rossner, P., 2019. Short-term and long-term exposure of the MucilAir™ model to polycyclic aromatic hydrocarbons. ATLA Alternatives to Laboratory Animals 47 (1), 9–18. https://doi.org/10.1177/0261192919841484.

Champion, J.A., Walker, A., Mitragotri, S., 2008. Role of particle size in phagocytosis of polymeric microspheres. Pharm. Res. 25, 1815–1821. https://link.springer.com/article/10.1007/s11095-008-9562-y#citeas.

Crespin, S., Bacchetta, M., Bou Saab, J., Tantilipikorn, P., Bellec, J., Dudez, T., Nguyen, T.H., Kwak, B.R., Lacroix, J.S., Huang, S., Wiszniewski, L., Chanson, M., 2014. Cx26 regulates proliferation of repairing basal airway epithelial cells. Int. J. Biochem. Cell Biol. 52, 152–160. https://doi.org/10.1016/j.biocel.2014.02.010.

Doke, S.K., Dhawale, S.C., 2015. Alternatives to animal testing: a review. Saudi Pharm. J. 23 (3), 223–229. https://doi.org/10.1016/j.jsps.2013.11.002.

Domenech, J., Villacorta, A., Ferrer, J.F., Llorens-Chiralt, R., Marcos, R., Hernández, A., Catalán, J., 2024. In vitro cell-transforming potential of secondary polyethylene terephthalate and polylactic acid nanoplastics. J. Hazard. Mater. 469, 134030. https://www.sciencedirect.com/science/article/pii/S0304389424006095.

Franz, P., Bürkle, A., Wick, P., Hirsch, C., 2020. Exploring flow cytometry-based micronucleus scoring for reliable nanomaterial genotoxicity assessment. Chem. Res. Toxicol. 33 (10), 2538–2549. https://doi.org/10.1021/ACS.CHEMRESTOX.0C00071/SUPPL_FILE/TX0C00071_SI_001.PDF.

Gandon, A., Werle, K., Neubauer, N., Wohlleben, W., 2017. Surface reactivity measurements as required for grouping and read-across: an advanced FRAS protocol. J. Phys. Conf. Ser. 838. https://doi.org/10.1088/1742-6596/838/1/012033.

García-Salvador, A., Katsumiti, A., Rojas, E., Aristimuño, C., Betanzos, M., Martínez-Moro, M., Moya, S.E., Goñi-De-cerio, F., 2021. A complete in vitro toxicological assessment of the biological effects of cerium oxide nanoparticles: from acute toxicity to multi-dose subchronic cytotoxicity study. Nanomaterials 11 (6). https://doi.org/10.3390/nano11061577.

Haswell, L.E., Smart, D., Jaunky, T., Baxter, A., Santopietro, S., Meredith, S., Camacho, O.M., Breheny, D., Thorne, D., Gaca, M.D., 2021. The development of an in vitro 3D model of goblet cell hyperplasia using MUC5AC expression and repeated whole aerosol exposures. Toxicol. Lett. 347, 45–57. https://doi.org/10.1016/J.TOXLET.2021.04.012.

He, R.-W., Braakhuis, H., Vandebriel, R.J., Staal, Y.C.M., Gremmer, E.R., Fokkens, P.H.B., Kemp, C., Vermeulen, J., Westerink, R.H.S., Cassee, F.R., 2021. Optimization of an air-liquid interface in vitro cell co-culture model to estimate the hazard of aerosol exposures. J. Aerosol Sci. 153, 105703.

Ito, S., Matsumura, K., Ishimori, K., Ishikawa, S., 2020. In vitro long-term repeated exposure and exposure switching of a novel tobacco vapor product in a human organotypic culture of bronchial epithelial cells. In. J. Appl. Toxicol. 40 (9), 1248–1258. https://doi.org/10.1002/jat.3982.

Jackson, P., Pedersen, L.M., Kyjovska, Z.O., Jacobsen, N.R., Saber, A.T., Hougaard, K.S., Vogel, U., Wallin, H., 2013. Validation of freezing tissues and cells for analysis of DNA strand break levels by comet assay. Mutagenesis 28 (6), 699–707. https://doi.org/10.1093/mutage/get049.

Jiang, T., Amadei, C.A., Gou, N., Lin, Y., Lan, J., Vecitis, C.D., Gu, A.Z., 2020. Toxicity of single-walled carbon nanotubes (SWCNTs): effect of lengths, functional groups and electronic structures revealed by a quantitative toxicogenomics assay. Environ. Sci. Nano 7 (5), 1348. https://doi.org/10.1039/D0EN00230E.

Karlsson, H.L., Cronholm, P., Gustafsson, J., Möller, L., 2008. Copper oxide nanoparticles are highly toxic: a comparison between metal oxide nanoparticles and carbon nanotubes. Chem. Res. Toxicol. 21 (9), 1726–1732. https://doi.org/10.1021/TX800064J.

Kisin, E.R., Murray, A.R., Sargent, L., Lowry, D., Chirila, M., Siegrist, K.J., Schwegler-Berry, D., Leonard, S., Castranova, V., Fadeel, B., Kagan, V.E., Shvedova, A.A., 2011. Genotoxicity of carbon nanofibers: are they potentially more or less dangerous than carbon nanotubes or asbestos? Toxicol. Appl. Pharmacol. 252 (1), 1–10. https://doi.org/10.1016/j.taap.2011.02.001.

Kohl, Y., Rundén-Pran, E., Mariussen, E., Hesler, M., El Yamani, N., Longhin, E.M., Dusinska, M., 2020. Genotoxicity of nanomaterials: advanced in vitro models and high throughput methods for human hazard assessment—a review. Nanomaterials 10 (10), 1–25. https://doi.org/10.3390/nano10101911.

Kooter, I.M., Gröllers-Mulderij, M., Duistermaat, E., Kuper, F., Schoen, E.D., 2017. Factors of concern in a human 3D cellular airway model exposed to aerosols of nanoparticles. Toxicol. In Vitro. https://doi.org/10.1016/j.tiv.2017.07.006.

Kristiawan, R.B., Rusdyanto, B., Imaduddin, F., Ariawan, D., 2021. Glass powder additive on recycled polypropylene filaments: a sustainable material in 3D printing. Polymers. https://doi.org/10.3390/polym14010005.

Kwon, O., Yoon, C., Ham, S., Park, J., Lee, J., Yoo, D., Kim, Y., 2017. Characterization and control of nanoparticle emission during 3D printing. Environ. Sci. Tech. 51 (18), 10357–10368. https://doi.org/10.1021/acs.est.7b01454.

Lisiecki, M., Belé, T., Ügdüler, S., Fiorio, R., Astrup, T., De Meester, S., Ragaert, K., 2024. Mechanical recycling of printed flexible plastic packaging: the role of binders and pigments. J. Hazard. Mater. 472.

Ludwicka, K., Kolodziejczyk, M., Gendaszewska-Darmach, E., Chrzanowski, M., Jedrzejczak-Krzepkowska, M., Rytczak, P., Bielecki, S., 2018. Stable composite of bacterial nanocellulose and perforated polypropylene mesh for biomedical applications. J. Biomed. Mater. Res. B Appl. Biomater. 107. https://doi.org/10.1002/jbm.b.34191.

Makki, T., Vattathurvalappil, S.H., Theravalappil, R., Nazir, A., Alhajeri, A., Azeem, M. A., Mahdi, E., Ummer, A.C., Ali, U., 2024. 3D and 4D printing: a review of virgin polymers used in fused deposition modeling. Compos. Part C Open Access 14 (May), 100472. https://doi.org/10.1016/j.jcomc.2024.100472.

Meindl, C., Absenger-Novak, M., Jeitler, R., Roblegg, E., Fröhlich, E., 2023. Assessment of carbon nanotubes on barrier function, ciliary beating frequency and cytokine release in in vitro models of the respiratory tract. Nanomaterials 13 (4). https://doi.org/10.3390/nano13040682.

Mercier, C., Jacqueroux, E., He, Z., Hodin, S., Constant, S., Perek, N., Boudard, D., Delavenne, X., 2019. Pharmacological characterization of the 3D MucilAir™ nasal model. Eur. J. Pharm. Biopharm. 139 (April), 186–196. https://doi.org/10.1016/j.ejpb.2019.04.002.

Metz, J., Knoth, K., Groß, H., Lehr, C.-M., Stäbler, C., Bock, U., Hittinger, M., 2018. Pharmaceutics combining MucilAir™ and Vitrocell ® powder chamber for the in vitro evaluation of nasal ointments in the context of aerosolized pollen. https://doi.org/10.3390/pharmaceutics10020056.

Miller, A.J., Spence, J.R., 2017. In vitro models to study human lung development, disease and homeostasis. Physiology 32 (3), 246–260. https://doi.org/10.1152/physiol.00041.2016.

OECD, 2023. *Test No. 487: In Vitro Mammalian Cell Micronucleus Test*, OECD Guidelines for the Testing of Chemicals, Section 4. OECD Publishing, Paris. https://doi.org/10.1787/9789264264861-en.

Pauluhn, J., Mohr, U., 2000. Inhalation studies in laboratory animals - current concepts and alternatives. Toxicol. Pathol. 28 (5), 734–753. https://doi.org/10.1177/019262330002800514.

Petersen, E.J., Elliott, J.T., Gordon, J., Kleinstreuer, N.C., Reinke, E., Roesslein, M., Toman, B., 2023. Technical framework for enabling high quality measurements in new approach methodologies (NAMs). Altex 40 (1), 174–186. https://doi.org/10.14573/altex.2205081.

Rackley, C.R., Stripp, B.R., 2012. Building and maintaining the epithelium of the lung. J. Clin. Invest. 122. https://doi.org/10.1172/JCI60519.

Ren, D., Nelson, K.L., Uchakin, P.N., Smith, A.L., Gu, X.-X., Daines, D.A., 2012. Characterization of extended co-culture of non-typeable Haemophilus influenzae

with primary human respiratory tissues. Exp. Biol. Med. 237, 540–547. https://doi.org/10.1258/ebm.2012.011377.

Rodríguez-Garraus, A., Passerino, C., Vales, G., Carlin, M., Suhonen, S., Tubaro, A., Gómez, J., Pelin, M., Catalán, J., Rodriguez-Garraus, A., Gomez C, J., Catalan, J., 2023. Impact of physico-chemical properties on the toxicological potential of reduced graphene oxide in human bronchial epithelial cells. Nanotoxicology 17 (5), 471–495. https://doi.org/10.1080/17435390.2023.2265465.

Rodríguez-Garraus, A., Venäläinen, M., Lyyränen, J., Pulli, H., Salmatonidis, A., Lotti, D., Domenech, J., Fernández, J.F., Guzmán-Mínguez, J., Isasi-Vicente, M., Katsumiti, A., Rodríguez-Llopis, I., Vázquez-Campos, S., Carrière, M., Catalán, J., 2025. In vitro cell-transforming capacity of micro- and nanoplastics derived from 3D-printing waste. Ecotoxicol. Environ. Saf. 293 (November 2024). https://doi.org/10.1016/j.ecoenv.2025.118007.

Rossner, P., Cervena, T., Vojtisek-Lom, M., Vrbova, K., Ambroz, A., Novakova, Z., Elzeinova, F., Margaryan, H., Beranek, V., Pechout, M., Macoun, D., Klema, J., Rossnerova, A., Ciganek, M., Topinka, J., 2019. The biological effects of complete gasoline engine emissions exposure in a 3D human airway model (Mucilairtm) and in human bronchial epithelial cells (BEAS-2B). Int. J. Mol. Sci. 20 (22). https://doi.org/10.3390/ijms20225710.

Rossner, P., Cervena, T., Vojtisek-Lom, M., Neca, J., Ciganek, M., Vrbova, K., Ambroz, A., Novakova, Z., Elzeinova, F., Sima, M., Simova, Z., Holan, V., Beranek, V., Pechout, M., Macoun, D., Rossnerova, A., Topinka, J., 2021. Markers of lipid oxidation and inflammation in bronchial cells exposed to complete gasoline emissions and their organic extracts. Chemosphere 281, 130833. https://doi.org/10.1016/J.CHEMOSPHERE.2021.130833.

Ruijter, N., Boyles, M., Braakhuis, H., Ayerbe Algaba, R., Lofty, M., di Battista, V., Wohlleben, W., Cassee, F.R., Candalija, A., 2024. The oxidative potential of nanomaterials: an optimized high-throughput protocol and interlaboratory comparison for the ferric reducing ability of serum (FRAS) assay. Nanotoxicology 18 (8), 724–738. https://doi.org/10.1080/17435390.2024.2438116;CTYPE:STRING:JOURNAL.

Schwarz, A., Ligthart, T., Godoi Bizarro, D., De Wild, P., Vreugdenhil, P., van Harmelen, T., 2021. Plastic recycling in a circular economy; determining environmental performance through an LCA matrix model approach. Waste Manag. 121, 331–342.

Shiva, S., Prabu G, A.R., Bajaj, G., Elsa John, A., Chandran, S., Vijay Kumar, V., Ramakrishna, S., Abstract, G., 2023. A review on the recent applications of synthetic biopolymers in 3D printing for biomedical applications. J. Mater. Sci. Mater. Med. 34. https://doi.org/10.1007/s10856-023-06765-9.

Sigloch, H., Bierkandt, F.S., Singh, A.V., Gadicherla, A.K., Laux, P., Luch, A., 2020. 3d printing - evaluating particle emissions of a 3d printing pen. J. Vis. Exp. 2020 (164), 1–15. https://doi.org/10.3791/61829.

Srinivasan, B., Reddy Kolli, A., Brigitte Esch, M., Erbil Abaci, H., Shuler, M.L., Hickman, J.J., 2015. TEER measurement techniques for in vitro barrier model systems. SLAS Technol. 20, 107–126. https://doi.org/10.1177/2211068214561025.

Stefaniak, A.B., Johnson, A.R., du Preez, S., Hammond, D.R., Wells, J.R., Ham, J.E., LeBouf, R.F., Martin, S.B., Duling, M.G., Bowers, L.N., Knepp, A.K., de Beer, D.J., du Plessis, J.L., 2019. Insights into emissions and exposures from use of industrial-scale additive manufacturing machines. Saf. Health Work 10 (2), 229–236. https://doi.org/10.1016/J.SHAW.2018.10.003.

Suzuki, G., Uchida, N., Tuyen, L.H., Tanaka, K., Matsukami, H., Kunisue, T., Takahashi, S., Viet, P.H., Kuramochi, H., Osako, M., 2022. Mechanical recycling of plastic waste as a point source of microplastic pollution. Environ. Pollut. 303.

Tratnjek, L., Sibinovska, N., Kristan, K., Kreft, M.E., 2021. In vitro ciliotoxicity and cytotoxicity testing of repeated chronic exposure to topical nasal formulations for safety studies. Pharmaceutics 13 (11). https://doi.org/10.3390/pharmaceutics13111750.

Vallabani, N.V.S., Alijagic, A., Persson, A., Odnevall, I., Särndahl, E., Karlsson, H.L., 2022. Toxicity evaluation of particles formed during 3D-printing: cytotoxic, genotoxic, and inflammatory response in lung and macrophage models. Toxicology 467. https://doi.org/10.1016/j.tox.2022.153100.

van der Zalm, A.J., Barroso, J., Browne, P., Casey, W., Gordon, J., Henry, T.R., Kleinstreuer, N.C., Lowit, A.B., Perron, M., Clippinger, A.J., 2022. A framework for establishing scientific confidence in new approach methodologies. Arch. Toxicol. 96 (11), 2865–2879. https://doi.org/10.1007/s00204-022-03365-4.

Velásquez-García, L.F., Kornbluth, Y., 2025. Biomedical applications of metal 3D printing. Annu. Rev. Biomed. Eng. 23, 31. https://doi.org/10.1146/annurev-bioeng-082020.

Wade, A.M., Peloquin, D.M., Matheson, J.M., Luxton, T.P., 2023. Dermal and oral exposure risks to heavy metals from 3D printing metal-fill thermoplastics. Sci. Total Environ. 903, 166–538. https://doi.org/10.1016/j.scitotenv.2023.166538.

Wāng, Y., Han, Y., Xu, D.X., 2024. Developmental impacts and toxicological hallmarks of silver nanoparticles across diverse biological models. Environ. Sci. Ecotechnol. 19, 100325. https://doi.org/10.1016/J.ESE.2023.100325.

Welch, J., Wallace, J., Lansley, A.B., Roper, C., 2021. Evaluation of the toxicity of sodium dodecyl sulphate (SDS) in the MucilAir™ human airway model in vitro. Regul. Toxicol. Pharmacol. 125 (April), 105022. https://doi.org/10.1016/j.yrtph.2021.105022.

Yang, Q., Dai, H., Wang, B., Xu, J., Zhang, Y., Chen, Y., Ma, Q., Xu, F., Cheng, H., Sun, D., Wang, C., 2023a. Nanoplastics shape adaptive anticancer immunity in the Colon in mice. Nano Lett. 23 (8), 3516–3523.

Yang, D., Yang, H., Shi, M., Jia, X., Sui, H., Liu, Z., Wu, Y., 2023b. Advancing food safety risk assessment in China: development of new approach methodologies (NAMs). Front. Toxicol. 5 (November), 1–10. https://doi.org/10.3389/ftox.2023.1292373.

Zhang, Q., Black, M.S., 2023. Exposure hazards of particles and volatile organic compounds emitted from material extrusion 3D printing: consolidation of chamber study data. Environ. Int. 182 (November), 108316. https://doi.org/10.1016/j.envint.2023.108316.

Zhou, X., Zhou, X., Wang, C., Zhou, H., 2023. Environmental and human health impacts of volatile organic compounds: a perspective review. Chemosphere 313, 137489. https://doi.org/10.1016/J.CHEMOSPHERE.2022.137489.